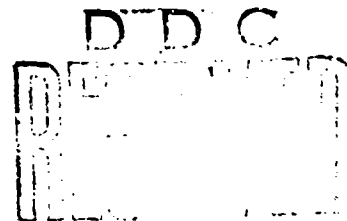# THE USE OF A LASER FOR ARPA MILITARY GEOPHYSICS PROGRAM (ROCK MECHANICS AND RAPID EXCAVATION)

FINAL TECHNICAL REPORT

AVCO EVERETT RESEARCH LABORATORY
a division of
AVCO CORPORATION
Everett, Massachusetts

D D C

Contract No. H0210039

October 1972

supported by

ADVANCED RESEARCH PROJECTS AGENCY
DEPARTMENT OF DEFENSE

monitored by

BUREAU OF MINES
DEPARTMENT OF INTERIOR

Details of illustrations in
this document may be better
studied on microfiche

DISTRIBUTION OF THIS DOCUMENT IS UNLIMITED

FOREWORD

Short Title of Work: The Use of a Laser for ARPA Military Geophysics Program (Rock Mechanics and Rapid Excavation)

ARPA Order Number: 1597

Program Code Number: 1F10

Name of Contractor: Avco Everett Research Laboratory

Effective Date of Contract: April 29, 1971

Contract Expiration Date: September 28, 1972

Amount of Contract: $73,280

Contract Number: H0210039

Principal Investigator and Phone Number: Dr. J. L. Zar, 389-3000, Ext. 225

Project Scientist or Engineer: Dr. J. L. Zar, 389-3000, Ext. 225

TECHNICAL SUMMARY

This is a study of the penetration and cracking of rocks using lasers available at the Avco Everett Research Laboratory. The objectives are: 1) to obtain data on the rate of rock damage for various laser conditions and 2) to present an analytical program to predict the temperature and stress in rocks for pointed and annular beams of radiation.

The laser power output used thus far was from 1 to 17 kW, CW, 10.6 microns and pulsed laser power up to 1000 joules in 20 microseconds. Data was taken with sharply focused as well as defocussed beams. Data is presented for continuous irradiation as well as pulsed, pointed beams and annular radiation patterns. Three types of hard rock were tested namely: quartzite, a Rhode Island granite, and Dresser basalt. Hole penetration energy per cm of penetration was found to be independent of laser intensity over 6 orders of magnitude. The specific energy for rock removal was found to depend on the fifth root of laser intensity over the same range.

A computer program was developed using the finite element method. It takes a radiation pattern, and delivers curves for thermoelastic strain and stress in any direction. This program is capable of working with high intensity laser radiation because it includes nonlinear heat conductivity, a temperature cut-off at the boiling point, anisotropic elastic conditions and a special iterative procedure to avoid computation instabilities resulting from too rapid heating. This program predicts that efficient cracking of rocks will be achieved by directing the radiation in a large annulus. The beam is moved so that the temperature of any point stays below the melting point. However, thermoelastic stress builds up in depth.

These predictions have been verified by experiments. However, the experiments to spall away basalt and quartzite consume more energy than predicted from the thermoelastic computer program. This is believed to be because the computer predicts the condition of crack generation whereas the experiments show the complete separation of rock material when the cracks are extended to a complete spall.

TABLE OF CONTENTS

Preceding page blank

LIST OF ILLUSTRATIONS

LIST OF SYMBOLS

λ Wavelength of light

f   Ratio of focal length to aperture of an optical system

k   Thermal conductivity

ρ Density

C   Specific Heat

α Linear coefficient of thermal expansion

ϵ Strain

T   Temperature (degrees C or K)

r   Radius

v Velocity

σ Stress

c   Velocity of sound

ν Poisson's Ratio

E   Elastic modulus

I. INTRODUCTION

This report is for the fourteen months of a study on penetrating and cracking rocks using a powerful laser. It is part of the ARPA Military Geophysics Program designed to develop improved methods for excavation, tunneling and rapid rock removal and is administrated through the Bureau of Mines, Department of Interior. Avco Everett Research Laboratory (AERL) has a contract to investigate the interactions using powerful lasers available at AERL.

The present contract does not concern itself with the construction or the development of the laser, but instead with the use of lasers in study ng the penetration and fragmentation of rock.

The program of work dealt exclusively with hard rocks. Three rock types, quartzite, basalt, and granite were selected by the Bureau of Mines. We were asked to determine how the laser produced hole drilling by melting and vaporization, rock fragmentation by cracking or spalling, and the effects of laser induced pressure.

It is clear that a powerful laser does not interact in a simple fashion with rocks or other materials. Unless the energy is properly controlled, most of it may be reflected or absorbed outside of the material and not produce a direct interaction. For example a great deal of energy is required for vaporization of rock in hole drilling with a laser, whereas much less energy would be required for cracking a large rock. Therefore, in parallel with experiments, a second and very important part of the program was to derive analytical methods for evaluating the interaction of the laser energy so that AERL can predict the resulting temperatures, mechanical stresses and cracks. In this way, it is hoped to create the largest possible damage to rocks for a given amount of laser energy. Theoretical analysis was done to support the experiments and computer calculations led to some interesting conclusions as will be described.

1

Even if rocks were rapidly excavated, this may not be the rate controlling step in the construction of a tunnel or an excavation. It often happens that the speed of excavation is controlled by factors such as the need to support the roof and sides of a tunnel or the control of water. Exploratory testing in advance of the excavation face is required. This is extremely time consuming and the results are often inclusive. Thus, excavation must proceed cautiously. If the laser can be used, in addition to rock excavation, for obtaining information concerning the consolidation of the formations ahead of the tunneling face or for determining the presence of underground streams, pools, etc. It would be extremely helpful in speeding up the excavation process. In the concluding part of this report there are some suggestions as to how the laser might be used for this purpose.

The analytical work that has been done under this contract is to examine how thermal elastic stress can be generated by a radiation of an annular region of a large rock face. The result of these calculations, using a computer, is that hard rocks can be spalled by a laser beam moving in a circular path over the rock with an intensity so that the surface remains below the melting point. After some period, tensile stresses are generated which are sufficient to crack rocks. Analytically, the energy required is of the order of 100 j/cm^3 for granite rocks and lower for the more easily spalled quartzite. When these experiments were done, it was found that an order of magnitude larger energy is required. We believe this is because the initial failure of the rock surface does not lead to complete rock removal. Additional energy has to be supplied until the crack grows large enough for the spalled region to be physically detached.

This compares also with about 450 j/cm^3 for a jack hammer and about 3,000 j/cm^3 for oil field drilling.[1] Since electric lasers have an efficiency, it is estimated, of about 20%, in the transfer of electric energy to light energy, the laser represents an attractive potential tool for excavation.

Modern, continuous flow lasers can be operated with either a pulsed or a steady output beam. It is very likely that if a rock face is cracked, and yet the boulders do not automatically fall out, one could design a laser

-2-

that could be switched to a pulsed condition and break these loose, if they do not fall out by themselves.

Thus, by a variety of methods, we feel that the development of laser tunneling could lead to a large degree of automation, increase in safety, increase in the speed of tunneling and reduction in cost.

II. DESCRIPTION OF LASERS AND EXPERIMENTAL CONDITIONS

With the development of gas lasers, it became possible to produce laser energy many orders of magnitude larger than was possible with solid or liquid lasers. This is primarily because it is possible to remove the heat generated in the gas by rapidly flowing the gas through the laser cavity. Furthermore, low pressure gas discharges, can be built in very large sizes because the gas remains optically homogeneous and virtually lossless at the lasing wavelength.

The most powerful lasers today are the CO_2: N_2; He lasers producing radiation at 10.6 μ. At AERL, these have been developed to a high degree of efficiency. All but a few preliminary experiments were done with continuous wave (C. W.) lasers. The highest power laser that we have used, producing 18,000 watts is called the Mark VB. The ionization of the lasing gas is produced directly from combustion. In this laser, there is a long focus optical system and the beam spot diameter is somewhat larger than the newer, electric lasers that were used for most of the work. The electric lasers have a maximum continuous power output of over 10,000 watts. Most of the experiments have been done with an f/6 Cassegrain telescope giving a very finely focused, diffraction limited beam spot. This will be further described below.

Figure 1 shows a typical laser optical system. The laser itself is contained within the region enclosed by the rectangle. The essential parts are a source of gas flow, a source of ionization which may be combustion, or an electrical discharge, etc. Finally there are mirrors for collecting the light in the optical cavity and bringing them through an aperture to the exterior of the laser. Outside of the laser, the beam can be controlled so as to reach a sharply focused spot on the target, a moving spot, or any other desired pattern. In one type of optical system, the beam is first collimated, then directed as a parallel beam to any other location, and finally focused on the target through a telescope.

Preceding page blank

PLAN OF LASER OPTICAL SYSTEM
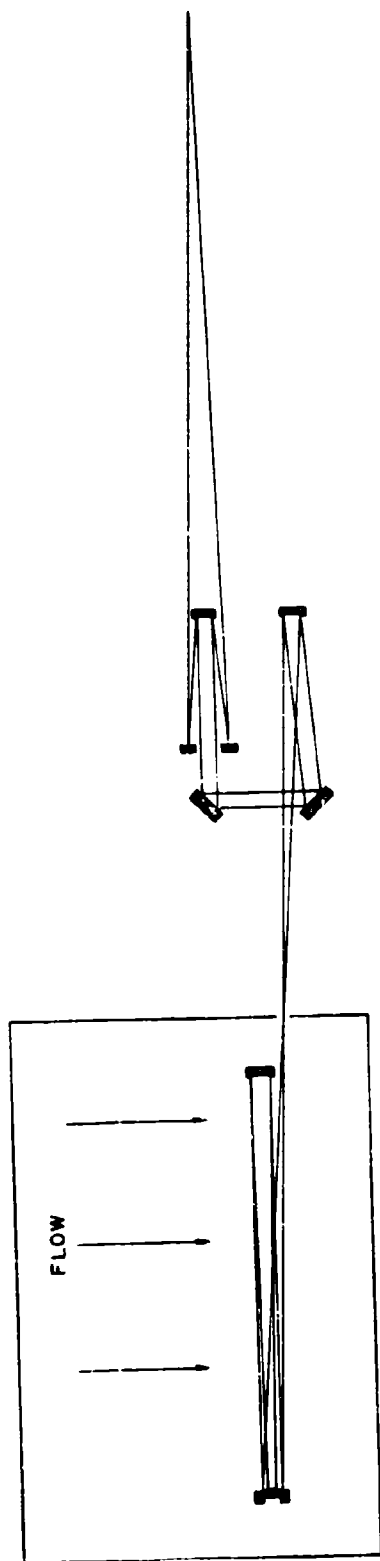
Figure 1   A typical laser optical system. The beam is brought thro a window, collimated, steered to any desired location an focussed on the target through a telescope.

In many of the experiments, the collimating system was omitted and the beam collected directly in the telescope and focused onto the target. For producing a circular moving spot of laser light, a mirror is inserted in the beam, after the telescope and this mirror is mechanically wobbled by a motor driven cam. For producing cuts such as kerfs, the rock speciman is mounted on a milling machine table with a driven feed screw. For some of the early work in which small rock specimens were used and some circular beams generated, the rock was mounted on a fixture and rotated by an electric motor eccentric to the laser spot.

The laser transition occurs between the 00^01 and the 10^00 vibrational levels of the carbon dioxide molecule. The energy difference between these levels corresponds to lasing wavelength of 10.6 microns, in the infrared. Nitrogen molecules in the discharge are excited by electronic collisions to the $\nu = 1$ level which can acquire an excess population. This energy is effectively transferred to the upper laser level in CO_2 which is thereby populated with an excess of molecules as compared to the lower laser level. After lasing, the CO_2 molecule subsequently radiates to the ground state. The helium in the discharge assists in collision processes which maintain the population inversion and improves the waste heat removal from the laser cavity. Within the cavity, are located the mirrors by which the laser energy is gathered and transmitted to the exterior of the cavity for experiments. These mirrors are designed so that single mode of operation is assured. The laser beam emerges from the device through a flowing gas window and is focused to the target by a pair of spherical copper mirrors arranged as a Cassegrain telescope, f/6. Samples may be placed about 1 meter from the telescope and 3 meters from the machine.

The intensity of the laser at a working surface is a function of the laser power and the spot size. The power is directly measured, whereas the spot size is determined from optical considerations.

For a circular laser source which fills the entire beam diameter, it can be shown that 84% of the energy falls within the diameter of the first dark ring of the Airy diffraction pattern.[2] This is a spot diameter given

by $d = 2.44 \lambda F$, where λ is the wavelength and F the focal ratio of the laser beam. A simple approach to the peak intensity would be to apportion the laser energy over the half width of the first Airy disc. For a 10,000 watt laser focused through f/6 optics the peak intensity is approximately $10,000 \text{ watts}/\pi(1.22 \text{ f } \lambda)^2 \times .84 = 4.5 \times 10^7 \text{ W/cm}^2$.

The laser systems used for these experiments employ an "unstable" resonator which emits an annular as opposed to a circular laser beam. The effect of an annulus is to redistribute a portion of the energy from the central part of the focal point to the "wings". This results in a larger focused beam size and a smaller peak intensity. We have evaluated the theoretical diffraction pattern for the type of laser that was used and an f/6 optical system. This gave an intensity at the peak of the pattern of $3.5 \times 10^7 \text{ W/cm}^2$, at 10,000 watts, slightly less than for a full circular beam, and proportionately higher for higher power. We would expect a beam half width of .008 cm.

In evaluating the peak laser intensity for experiments, the laser power is first multiplied by the amount of power contained in the first diffraction ring and this is then evaluated over an area representing the half power points of the first diffraction maximum. The assignment of these calculated values to the beam spot size was verified by two experiments in which the diameter of the tip of a short hole in rock was measured. While doing Test 32 the laser beam was allowed to cut a track in a block of quartzite and pass off the edge. The side view of this track was then examined with microscope. It is shown in Figure 2 at a magnification of 20 times. The bottom of the track is about .011 cm wide about the same as the theoretical width. In another experiment, Test 31, the profile of the track was obtained by passing the laser beam across two blocks of basalt tightly clamped together. When the rocks were separated the bottom of the cut could be seen as .01 cm. As a result of these tests, we believe that our optical systems are "near diffraction limited".

In observing the penetration of rocks the hole is drilled by the first maximum. The energy in the rings tends to widen the hole by cutting away at the sides. This produces a typical slightly tapered shape.
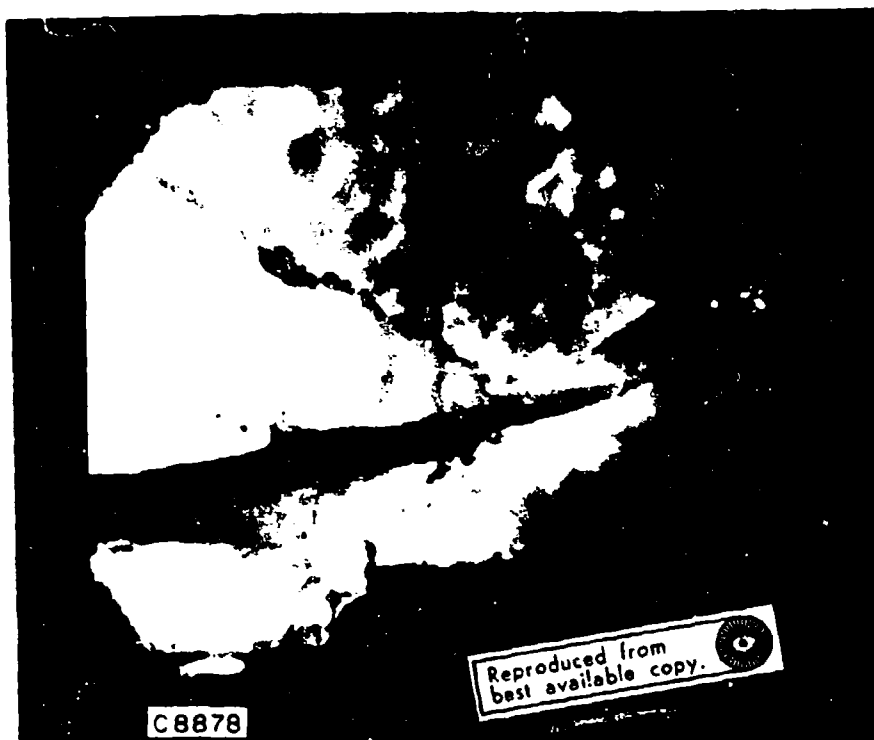
Figure 2   Track in a quartz block (Figure 3) viewed from the
side at 20 x magnification.   On the original photograph
the cut is seen to be 0. 1 mm wide.

The procedure that was used during the laser experiments was to position the specimen by using a small He Ne laser spot to align the rock with the principal beam. The power of the radiation was obtained from a recording of a calibrated power meter, or from a calibration curve based on sustainer current and voltage. The actual exposure was recorded on motion picture film. We could then count frames and observe the actual duration of the laser. Furthermore, when rocks were completely penetrated, this occurrence could be seen in the motion pictures by sparks appearing from the back side of the rock. In some of the experiments, the beam was controlled by a moving shutter. In this case, exposure times were obtained from the shutter control.

After the exposure, the rocks were examined. If possible the hole was probed with wires to determine the profile. In those cases where the rock was moved with respect to the beam, leaving a track, the profile of the track was obtained by taking a casting, sectioning it and observing the shape with a projection microscope. In other cases, when the volume of rock removed was to be determined, the cavity was filled with fine sand which could then be weighed.

Description of Rock Samples

The Bureau of Mines has requested that AERL use rocks from three specific quarries so that a comparison with other experiments can be made. The lab purchased quartzite from the Jasper Stone Company, Sioux City, Iowa. This was cleaved in blocks about 65 mm thick and later some of these were sawed to 25 mm thick. The source for granite was the Bonner Monument Company, Westerly, Rhode Island. This granite is light in color with small flakes of dark blue or black. The basalt was a dense variety, free from cracks, inclusions, etc., and was obtained from the Bryan Dresser Trap Rock Quarry, Dresser, Wisconsin.

III. DESCRIPTION OF EXPERIMENTS

Pulsed Experiments

Only one very short pulse experiment was done using a 1 joule pulsed laser which generated a 100 μsec beam with f/17 optics. The spot was 0.3 mm in diameter. The peak flux was 10^7 w/cm^2.

Two blocks of Jasper quartzite approximately 5 cm x 8 cm x 10 cm were exposed. The first was smoothed with a diamond saw so that the short scale roughness was less than 0.1 mm. The second was exposed in its cleaved condition. A single pulse of laser intensity produces a small pit on the surface of the rock. However, there was not sufficient energy to crack the rock. It did spall in a rather small region of the specimen. The cleaved sample was also exposed to a series of five pulses about 2 minutes apart, all focused at the same location, to see whether a hole could be drilled. Instead of a hole, a shallow crater was created which was considerably larger in diameter than depth. The volume of material removed was estimated with a microscope to be 7.4 x 10^{-4} cm^3. The calculated energy required to vaporize this volume of material is 15.7 joules, or about three times the available flux. We conclude, therefore, that pulses as short as 100 μsec are not absorbed in the body of the material. The material spalls and the particles carry away most of the laser flux, either by absorption, reflection, or the production of a small plasma. Laser pulses should therefore be longer in duration than 100 μsec. Other evidence that very little of the energy was imparted to the rock was the fact that the region surrounding the crater showed no evidence of melting and thus was not raised to the melting point.

However, we can derive information for millisecond length pulses from the experiments that were done with the continuous wave laser. From the profile of the track, obtained by inspection of castings, we calculated the volume of material that would be removed by a single pulse producing

a circular hole with the same profile as the track width. The pulse time is simply the track width divided by the velocity. In this way, the equivalent laser radiation for pulses was obtained.

In the case of circular tracks, the laser irradiated the same place a large number of times. The frequency is given by the reciprocal of the rate of revolution. Here, each individual pulse is much shorter because the velocity of travel in the circular track is much larger than for linear tracks. These experiments give us data for multiple pulses. The results are entered in Table II where appropriate.

Test Numbers 1, 2 and 3

The first three experiments that were done with the continuous wave laser are now described:

A block of quartzite, about 2.5 cm thick, was exposed to laser power of 5 kw focused in a small spot. In 1 second, a clean hole was bored through the quartz, striking a steel backing plate behind it. The hole diameter in the quartz was larger than the spot size. It was estimated to be 0.22 cm diameter by 2.3 cm long. Surrounding the hole there was a melted region and the rock itself had three fairly large cracks. Later, the energy was focused on one of the cracks. The rock literally exploded into four large pieces plus a great many small ones. The central area that had been fused by the original laser fell out intact as a fused quartz pipe. The time of exposure to the second laser impulse was not observable. It was so short that there was no evidence of any heating or melting of the rock. Now that the original fused pipe was available, we could estimate the amount of energy that had gone into melting and vaporizing. This came out slightly larger than our estimate of the incident energy, but within the roughness of our measurement, very much consistent. Therefore, we have concluded that in the case of quartzite a 5 kw steady state beam capable of vaporizing a hole interacts substantially completely with the material. A second conclusion is that energy focused on a crack releases sufficient

pressure beneath the surface so that fusion and vaporization does not occur. The result is a miniature explosion and is far more efficient in cracking rock.

A piece of granite was used for a third experiment about the same size as the quartzite and was exposed to the same power and the same size spot. The exposure was 6 seconds, some 30,000 joules. The result was one long crack and a hole about 2/3 the diameter of the one in the quartzite and only 1.8 cm deep. The granite material that was removed from the hole seemed to be collected at the rim and not vaporized. There was only a very thin melted zone around the hole. The appearance of the rock is shown in **Figure 3**. We estimate that 10 percent or less of the incident laser energy interacted with the granite. This effect is extremely interesting because of the very great difference in behavior between these two hard rocks. There is a slight difference in heat conductivity but we do not think it can account for a factor of 10 in the interaction.

The most likely explanation for the very different interaction of the laser with granite and quartzite is that the quartzite, being substantially a pure material, absorbs laser energy, dissociates at about 2500° K into silicon plus oxygen leaving a fresh quartz surface for irradiation. Thus, all of the laser energy interacts with the quartz. Granite, on the other hand, is an impure material, containing several percent of potassium and sodium. There is more than enough of these easily ionizable substances to generate a sufficient density of electrons in the vapor plume so as to reflect most of the laser energy before it strikes the rock. Thus except for certain pure minerals, effective laser interaction suggests that the energy should be introduced below the surface, in an existing crack or hole.

Test Number 11

This experiment consisted of exposing a quartzite block, about 2.5 cm thick, to a laser beam of 11 kW intensity, continuously. At first, the beam was allowed to fall on the stationary block. Examination of the motion pictures that were taken shows a large spall occurred after 1.25 seconds. At
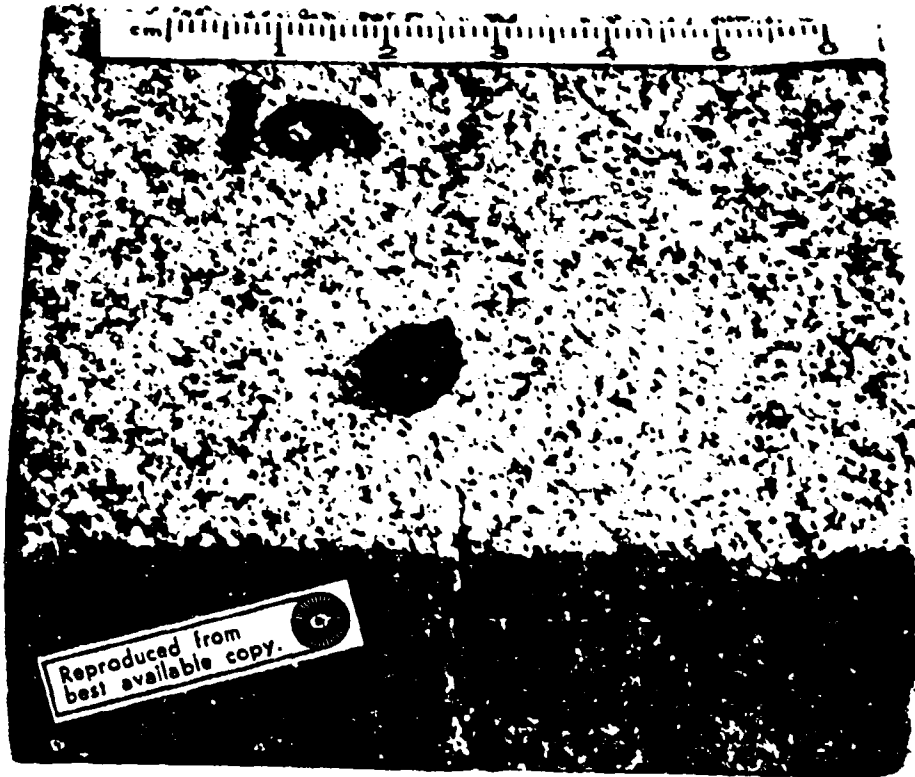
C 8882

Figure 3   Exposure of a 25 mm thick granite block to a 5000 watt
laser beam for 5 seconds.   This resulted in a hole,
1. 55 mm in diameter and 18 mm deep, and a thermal
crack.   When compared to the quartzite block, Figure 5,
this shows that the interaction with granite is very much
less than with quartzite.

1.8 seconds, the rock developed four large cracks, although it did not fall apart. The laser beam was stationary for the first 2.1 seconds. Then the block was moved through the beam at a rate of 2.1 cm/sec.

The initial stationary exposure resulted in a fine hole drilled through the quartzite in addition to the cracks. The subsequent motion of the block resulted in a cut about .7 cm deep with considerable melting at the surface and spalation of the material. A photograph of the rock after exposure to the laser is shown in Figure 4.

There are a number of observations that can be made as a result of this test. By direct probing we found that the initial hole drilled during the 2.1 seconds just barely penetrated the block thickness (2.8 cm). The amount of material vaporized was .0103 cm^3. From a number of observations of holes in quartzite we found that the amount of material molten is about 2.5 times the diameter of the material vaporized. This enabled us to calculate the energy that was transmitted to the rock. For example, the vaporization takes about 4.75×10^4 j/cm^3. Most of this energy is used in dissociating the SiO_2 at the sublimation temperature of $2500^\circ K$. In addition, the molten material absorbs 5000 j/cm^3 in its specific heat and latent heat. If an estimate is made that 2.5 times the diameter was molten as compared to the diameter vaporized, we conclude that the quartzite absorbed 7.38×10^4 j/cm^3. Of this amount, about two-thirds was used in vaporization. Thus, the hole in this test block, which had a volume of .0103 cm^3 required 760 joules for its formation. This is compared to the laser energy of 23,100 joules during the time of exposure. Quartzite, in this experiment used about three percent of the laser energy. The remainder was evidently absorbed by flying particles, vapor and general reflection. Motion pictures of the exposure clearly showed an incandescent plume.

After the rock began to move, the beam passed straight across the entire face. Examination of the end face shows the track left by the laser beam. A photomicrograph of the bottom part of this track is shown in Figure 2, enlarged 20 times. From this we observe firstly; that the beam

-15-

C8879
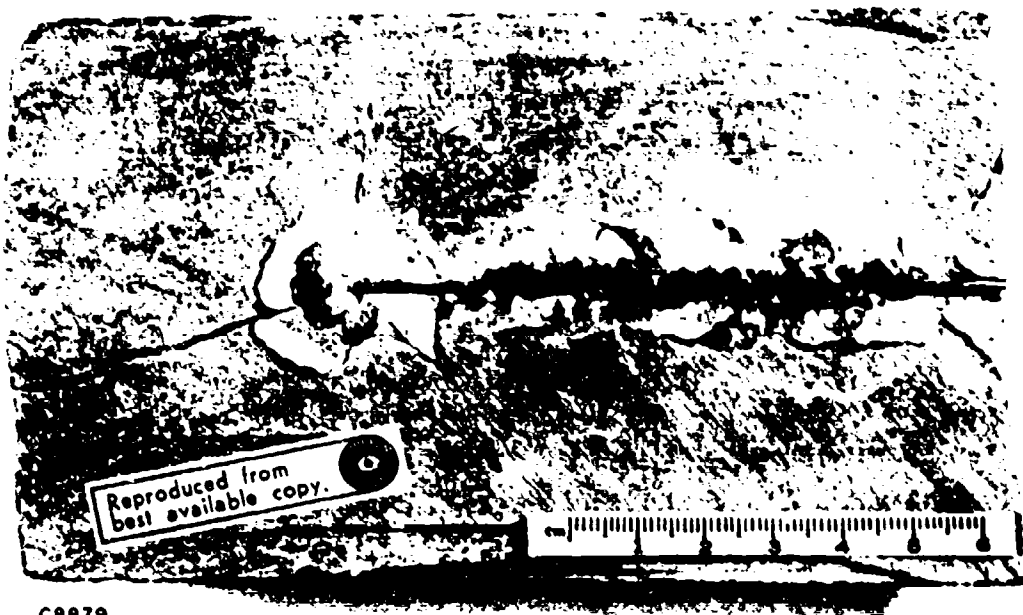
Figure 4   A quartz block, 25 mm thick exposed to a continuous
laser beam of 11 kW.   The beam penetrated the block
in 2.3 seconds and produced the series of cracks.
The block was then moved through the beam producing
the cut (Experiment No. 11).

was near diffraction limited. At the bottom of the slot, the beam was
.011 cm diameter whereas the theoretical spot size is .017 cm for f/6
optics. Furthermore, the area of the total gash that was cut in the rock
was measured with a mechanical stage microscope and found to be .095 cm^2.
Thus, we have a volume swept out during the exposure of .2 cm^3/sec.
This required an energy absorption, based on the above figure of 4.75×10^4 j/cm^3
of 9.5 kw. This checks with the available beam power of 11 kw. The moving
spot evidently did not generate a sufficiently intense plume to cause signifi-
cant absorption of the laser energy. Fresh material was constantly being
introduced so that the vapor temperature was lower than in the case of a
stationary exposure. This checks with the result obtained in Test 1 with a
5 kw beam in which, apparently, the full energy of the laser was absorbed
in generating a shallow hole or cut.

Test Numbers 12 and 15

These were two exposures of a 6.3 cm thick block of quartzite using
an 11 kw laser. The spot was focused on the surface and the specimen was
stationary. In Test 12, the exposure was 1.46 seconds. A 2.3 cm deep hole
was drilled, nearly straight sided, about .075 cm in diameter. The volume
of material removed was determined by probing with gauges and was
.0102 cm^3. This corresponds to an interaction energy of 750 joules. How-
ever, the incident laser energy was 15,300 joules giving an efficiency of
interaction of five percent. In Test 15, the block was exposed for 3.9 sec-
onds. A hole 4.8 cm deep was drilled and the volume of material removed
was .0356 cm^3. This same type of evaluation as for Test 12 gives 6.1 per-
cent of the incident laser energy interacting with the rock.

The conclusions of these tests are that the laser interacts with quartz-
ite of the order of five percent which is a rather low value. The hole depth is
linear with time of exposure within the range that was tested. This is not
surprising considering that the holes are very nearly straight sided and

-17-

narrow. What is surprising is that holes could be drilled about 5 cm deep with a diameter of the order of .1 cm. In 5 cm the beam would diverge .8 cm because the optics is f/6. Except for the small region near the very top of the hole, there was substantially no divergence. This is explained by the fact that the beam was reflected from the sides of the molten rock at nearly grazing incidence and does not have an opportunity to diverge or to dissipate. Instead it is channeled down the hole as a very narrow beam and presumably can continue much deeper than one would expect merely from an observation of the geometrical optical path.

Test Numbers 13 and 14

Test 13 was done with granite and Test 14 with basalt. The laser beam was 11 kw continuous, stationary, focused on the surface of the block, and left on for about 3 seconds. The result in granite and basalt was a fairly large diameter molten region, extending clear through the block, approximately .3 cm in diameter. There was a small hole in the granite of irregular shape. The hole in basalt was completely filled with molten material, although undoubtedly of low density. From an examination of the film it is possible to tell the time when the beam completely penetrated the blocks by the fact that sparks emerged from the rear side. The time was 1.25 seconds for granite and 0.85 seconds for basalt. The block thickness in both cases was 2.5 cm. Thus, the penetration rate was somewhat faster in basalt. It is not possible to estimate the degree of interaction of laser energy with the material because the holes were refilled with molten rock.

Test Numbers 16 and 17

These were exposures of 2.5 cm blocks of basalt and granite respectively. The laser power was 10 kw, continuously. The beam was sharp and focused onto the surface. Examination of the films indicate that the basalt was penetrated in 1.5 seconds leading to a penetration rate of about 1.7 cm/sec. The granite was penetrated in 1.1 seconds with a penetration rate of 2.3 cm/sec.

Test Number 18

This was a quartzite block 6.3 cm thick. The laser spot was focused approximately 1.2 cm beneath the surface of the rock so that the spot diameter was .21 cm. This had the effect of reducing the surface intensity. The exposure was 2.5 seconds to a beam power of 11 kw. Shortly after the exposure, the rock cracked into pieces and the hole, with a thin crust of molten material, was exposed so that the volume that was vaporized and the volume that was melted could easily be seen. This is shown in Figure 5. In this case, the melted diameter was 1.5 times the diameter of the vaporized zone. The total depth of the hole was 5.7 cm. This indicates a penetration rate much faster than for Test 12 and 15 and is attributable to a higher degree of laser coupling with the surface of the result reduced incident intensity. The total energy was 27,500 joules. Based on the dimensions of the hole, the energy used in vaporization was 5330 joules. Also, an additional 700 joules is estimated to have been used in the material that was melted around the hole. Thus, a total energy of 6000 joules can be accounted for. This represents 22 percent of the incident energy and is considerably higher than the five to six percent that was found in Test 12 and 15. It is therefore clear that in the case of quartzite, much higher energy coupling is attained with lower surface intensity when one has lasers with the power that was used in these experiments.

Test Numbers 19 and 20

These represent exposures of 2.5 cm thick blocks of granite and basalt to the same energy beam and the same degree of defocusing as already described in Test 18. It is estimated that the rock was burnt through in 0.83 seconds for basalt and in 2.33 seconds for granite representing a penetration rate of 3.0 cm/sec for basalt and 1.1 cm/sec for granite. In the case of granite, a small hole about .25 cm diameter resulted with a small melted zone around the edge. The total exposure was 3.3 seconds. The hole size
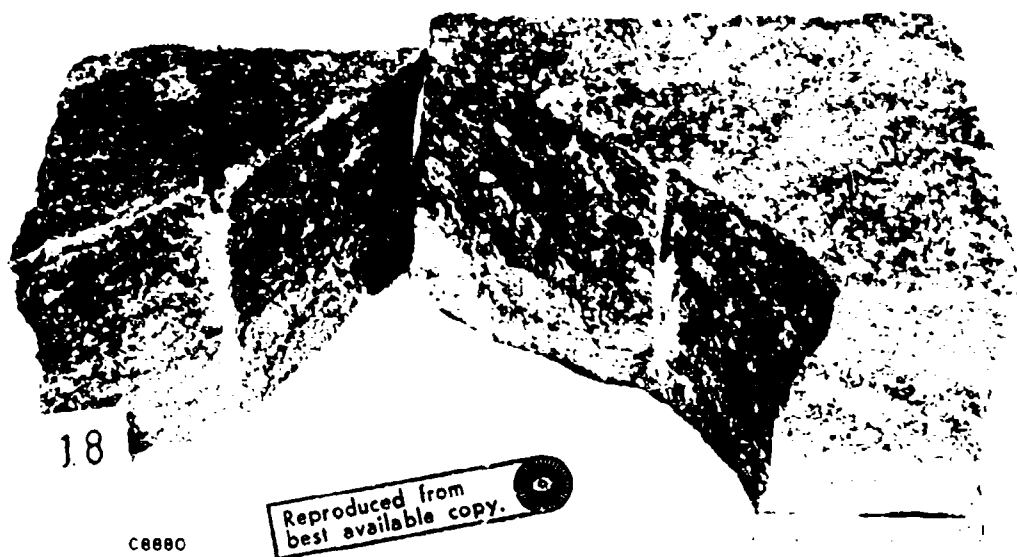
Figure 5   A quartzite block 6. 3 cm   thick.   The laser was focused
approximately 1. 2 cm below the surface.   This hole was
drilled in 2. 5 seconds at $11 kW$ and caused the crack in
the block.

in granite was .6 cm in diameter and there was a considerable amount of
molten material around the edge. It is quite clear then that with this sur-
face flux, much higher coupling is obtained in basalt than in granite. When
comparing the rate of penetration of Tests 19 and 20 with Tests 16 and 17,
where the beam was in a sharp focus but the energy was the same, we find
that the rate of penetration was higher with a lower intensity for basalt but
roughly the same in both granite tests. This contrasts very sharply with
the comparison of the same conditions for penetration rates in quartzite.

Test Numbers 21 Through 24

These experiments were done with rocks rotating at the rate of
400 rpm. The laser beam was directed 2.5 cm from the center of rotation
giving a circular annulus of radiation 50 mm in diameter. The incident
flux was 11,000 watts, continuous wave. In Test 21, 23 and 24 the spot was
focused on the surface of the rotating rock. These were quartzite, basalt,
and granite in that order. Test 22 was also quartzite but the laser spot was
focused beneath the surface giving an incident spot .21 cm diameter. We
will first discuss Tests 21, 23 and 24 in order. In all three cases, a groove
about .05 cm in width was cut into the rock. The volume of material that
was removed by the laser was observed by making a casting from the
groove, sectioning the cast, and obtaining a profile with a projection micro-
scope at 20 times 𝑟   tion. The number of joules per cubic centimeter of
material removed   quartzite, 4.8×10^4; 2) basalt, 1.9×10^5; 3) granite,
9.8×10^4. The valu   artzite agrees very closely with the value that is
estimated from the k..   physical constants for the vaporization of quartz. Exam-
ination of the groove shows just the smallest amount of melting. It is concluded
therefore that the moving spot is completely coupled with the quartzite and
the energy was efficiently transferred. However, basalt and granite grooves
showed considerable melting and had a much higher specific energy consump-
tion. This indicates that laser energy was absorbed or reflected even during
the very short local exposures that result from spot movement. This is con-
sistent with our previous observations using stationary laser beams. The
rate of penetration of the laser into the material was also in the same order
as the efficiency of radiation usage. Under the sharply focussed beam the

groove penetration rate in quartzite was .034 cm/sec of exposure; in basalt, .015 cm/sec, and in granite, .02 cm/sec.

Test 22 differed from the three preceeding ones in that the laser spot was broadened into a 0.2 cm wide beam. The track left by the laser was a shallow groove slightly wider than the beam width showing no evidence of melting. This is shown in Figure 6. Specific energy consumption was .029 j/cm^3 of quartzite removed, representing approximately 1.6 times the efficiency compared to vaporization. The penetration rate was .025 cm/sec notwithstanding the fact that the track was much wider than the concentrated beam. This is taken as evidence that the principal removal mechanism was spalling.

This experiment also enables us to determine the specific energy consumption for pulsed laser radiation. Since we know the track width and the velocity of motion, their quotient is the time of exposure of a particular spot on the rock to a pulse of radiation. From the profile of the track, we can determine, by graphical integration, the volume of material removed. This calculation was done for the data presented in Table II. Where the intensity is low on quartzite, the efficient principal removal mechanism was by spalling. In the case of basalt and granite tracks, there is evidence of melting and these gave higher specific energy consumption. Where the intensity is low on quartzite, the efficient principal removal mechanism was by spalling. In the case of basalt and granite tracks, there is evidence of melting and these gave higher specific energy consumption.

Test Numbers 32 Through 34

These three experiments were exposures of 6.3 cm thick blocks of quartzite to radiation from 11.5 kw continuous laser. The focal point was below the surface of the quartzite giving three different spot widths. The velocity of motion of the specimen was .33 cm/sec. The rock showed a

C8881
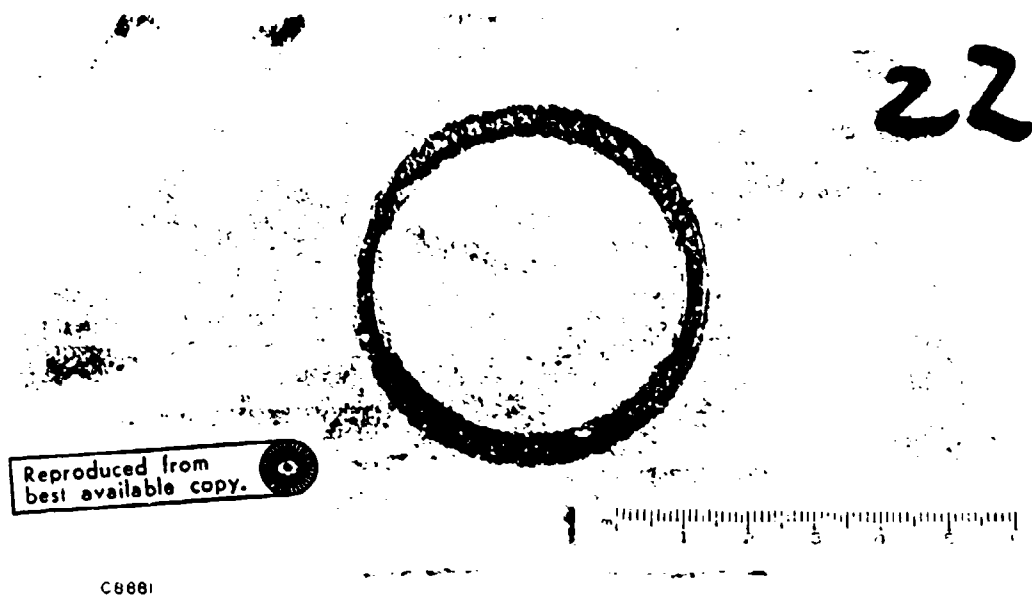
Figure 6   This block of quartzite was rotated at 400 rpm in an
11 kW laser beam which was focused beneath the sur-
face giving a spot width of . 21 cm in diameter.   The
exposure lasted 2. 5 seconds.   The track was . 15 cm
deep and showed no evidence of melting.   The efficiency
of cutting was . 029 j/cm^3 rock removed.

scar less than half the width of the geometric construction of the spot. This shows that for the defocused laser beam, the energy is primarily within the first diffraction pattern. No evidence of melting was found. The profile of the track was obtained by preparing a casting, sectioning it and examining the shape with a projection microscope. The duration of the exposure on the rock was obtained from the motion picture record. Thus, the effectiveness of the laser radiation could be determined. The data for these three experiments is given below:

	Test Number (Quartzite)		
	32	33	34
Depth of Focus Below Surface (mm)	185.	380.	89.
Spot Width (cm)	3.1	6.3	1.5
Track Width (mm)	14.	25.	9.
Area Removed (cm^2)	.361	.499	.385
Track Length (cm)	12.3	12.3	12.3
Volume of Rock Removed (cm^3)	4.440	6.140	4.740
Joules of Exposure	43,000.	42,500.	42,000.
Joules per cubic centimeter	9700	6900	8900

Here we see that there was insufficient energy available for melting the rock and in fact the examination of the track shows no evidence of melting. The profile of two of the tracks is given in Figure 7.

The test data also enables us to determine the amount of material removed for pulses of the order of a half second. The data is presented in Table 1 and the conclusion is that about 100 to 150 joules is required per centimeter of material spalled away. This is somewhat higher than the specific energy for much shorter pulses. With very low intensity, part of the heat is conducted into the interior of the block without causing large thermal stresses. Temperature diffuses into quartzite at a rate of about

-24-

TEST NO. 32

TEST NO. 34

C8949

Figure 7. Profile of two tracks cut in a block of quartzite by the laser beam magnified 10 times (Tests 32 and 34). Power was 11.5 kW, spot widths were 3.1 and 1.5 cm. The beam moved across the rock face at a velocity of 3.3 cm/sec.

.1 centimeter in a second and scales with the square root of t. In a half second, the laser heat is dissipated in .07 cm. Since the spalled region is several millimeters in width and depth, thermal diffusion is not the principal factor in explaining the high specific energy consumption. Very likely, the lower efficiency results from the very low surface intensity of the laser radiation, of the order of .5 w/cm^2.

Test Numbers 31, 35 and 36

These were tracks cut in 2.5 cm thick blocks of basalt by the same laser as previously described. In Test 31, the spot was focused on the surface of the rock. Two rocks were tightly clamped together so that a profile could be obtained of the shape of the laser spot in the material after the exposure. All three tracks showed considerable melting plus some spalling. The velocity of motion for Test 31 was 4.6 cm/sec. For Tests 35 and 36 it was 1.93 cm/sec. Data for the three experiments are listed below:

	Test Number (Basalt)		
	31	35	36
Depth of Focus Below Surface (cm)	0	8.9	18.5
Spot Width (cm)	.01	1.4	3.1
Track Width (cm)	.23	.9	1.5
Area Removed (cm^2)	.073	.147	.191
Track Length (cm)	20.2	10.4	10.4
Volume of Rock Removed (cm^3)	.148	1.53	1.97
Joules of Exposure	51,000.	61,000.	63,000.
Joules per cubic centimeter	1.13×10^5	4.0×10^4	3.15×10^4

It is apparent that the amount of energy absorbed by the basalt is considerably larger than that absorbed in quartzite for the same volume of material in the track and also that the efficiency of utilization of laser energy increases for lower intensity of exposure.

The tracks from basalt can be analyzed to give information about the pulsed laser beam. The three tracks have roughly the same specific energy in terms of joules per cubic centimeter of material removed although, there is a difference of five orders of magnitude in the beam intensity. Of greater interest is the comparison between the specific energy for basalt and for quartzite. The basalt uses about three to five times as much energy per cubic centimeter. This is additional evidence of the absorption of the laser beam in the plume above the surface.

Test Numbers 37 and 38

These were tracks cut in a 2.5 cm thick block of granite with a defocused laser spot and a track velocity of 1.87 cm/sec. The granite showed both melting and spalling. The photographs taken during the exposure for the granite tests as well as the basalt tests previously described showed that a large amount of smoke was given off. Also, we found that the energy used per unit volume of cut was quite large in the case of both the granite and basalt tests. The conclusions to be drawn from these tests on granite and basalt are that the beam energy available is larger than the maximum that could be used efficiently in cutting tracks in these rocks. That is, we are beyond the maximum curve of specific energy per cubic millimeter of rock removed.

	Test Number (Granite)	
	37	38
Depth of Focus Below Surface (cm)	18.5	6.4
Spot Width (cm)	3.1	1.05
Track Width (cm)	1.3	.65
Area Removed (cm^2)	1.13	.096
Track Length (cm)	77.5	77.5
Volume of Rock Removed (cm^3)	1.010	.740
Joules of Exposure	48,900.	46,500.
Joules per cubic centimeter	4.83×10^4	6.29×10^4

The results of the evaluation of pulses for granite are very similar to that obtained for basalt.

Test Number 51

This was the exposure of a basalt block 2.5 cm thick to a laser beam focused on the surface. The power was 1.25 kw. The block was penetrated in 2.7 seconds giving a rate of penetration of 1250 j/cm. However, the power was left on for a total of 9.3 seconds. At 7.5 seconds the rock cracked completely through. It was now possible to examine the cavity cut by the laser. About .1 cm^3 was burnt out, representing 10^5 j/cm^3 of rock removed. It is possible however that the actual efficiency was higher since the beam did pass through the rock and some of the energy must have been dissipated behind it.

Test Number 52

This was the exposure of a 2.5 cm thick block of granite, again to a 1.25 kw beam focused on the surface. The exposure was 11.2 seconds and the penetration was 2.4 cm, or 5850 j/cm. In this case, the rock cracked about halfway through. We completed the crack with a small blow, so that

the damaged section was exposed, and found that .06 cm^3 was cut out by the laser. This represents 2.33×10^5 j/cm^3 and in this case, it was all absorbed in or ahead of the rock.

Test Number 53

This was a block of basalt, 2.55 cm thick which was exposed to a 5.1 kw beam focused on the surface. In this case, the rock was burnt through in just 1.25 seconds. The total exposure time was 2.5 seconds controlled by a shutter. It was not possible to evaluate the damage because the rock cavity was filled with molten material. However, the penetration rate was 2300 j/cm. This is about half as efficient as 1.25 kw laser beam and indicates that with basalt, 5 kw is above the maximum efficiency of energy utilization for penetration.

Test Number 54

This was a penetration test in a thick block of quartzite with a 5.1 kw laser beam focused on the surface. The exposure was for 1 second timed by a shutter. The beam penetrated 1.9 cm, or 2780 j/cm. In this case, the hole was clean enough so that its size and depth could be determined by probing with fine wires. We found that .0062 cm^3 of quartzite was evaporated giving a specific energy consumption for penetration of quartzite of 8.2×10^5 j/cm^3. When compared with the theoretical value of 7.4×10^4 j/cm^3, we find that the laser interacted about nine percent with the rock.

Test Number 55

This test was identical to Test 54 however, the exposure was 2 seconds. The penetration was 4.3 cm giving an energy of 2370 j/cm. Once again the volume of the material that was vaporized was determined as .0155 cm^3 or 6.6×10^5 j/cm^3.

Test Numbers 56 and 57

These were exposures of a block of quartzite focused on the surface. The first exposure was to a 5.1 kw beam for 4 seconds which drilled a hole. Then after a few seconds during which the rock cooled the radiation was turned on again at the level of 10 kw for 1 second. The radiation was here much more effective. The quartzite rock had a fairly large crack in it, although not sufficiently deep to penetrate the full block which was 6.3 cm thick. The total penetration was 4.75 cm. However, the radiation that was consumed was 30,400 joules giving a penetration rate of 6400 j/cm. This is about half the penetration rate previously observed with quartzite. At present, we have no explanation for the low rate of penetration in this particular exposure.

Test Number 58

This was an exposure of 2.5 cm thick block of granite with radiation focused on the surface. The radiation level was 1 kw, for 6 seconds. The penetration was 1.1 cm giving 5400 j/cm. This is very similar to the value obtained in Test 52 with substantially the same power level, but half the exposure time. The hole was filled with molten granite so that it was not possible to determine its volume.

Test Number 59

This test was an exposure of a block of granite to 10 kw radiation focused on the surface. The block was 2.5 cm thick and burnt through in 0.79 second. This gives a penetration rate of 3170 j/cm. A comparison with Tests 52 and 58 shows a higher efficiency of utilization of laser energy. This indicates that the initial rate of penetration is probably faster before a large screen of smoke has been established.

Test Number 60

The next group of tests (Tests 60 through 68) were done with rocks rotating in the laser beam to create an annulus of radiation. Test 60 was a

quartzite rock turning at 460 rpm and exposed for 6.5 seconds to a beam 10.8 kw intensity. The beam was focused on the surface of the rock and cut a track in the rock 4.7 cm in diameter. The amount of material removed was obtained by examining a casting made from the track. It showed 3.71 cm^3 removed or a specific energy of 1.89 x 10^4 j/cm^3. Examination of the rock showed no evidence of melting. A rather wide V-track was spalled out and, of course, the energy per unit volume is much too low to allow for vaporization.

The same data was analyzed in terms of a pulsed beam with a frequency of 7.7 per second. Each pulse lasts 7.9 msec and in terms of the amount of material removed, an energy consumption of 4000 j/cm^3 is used. This is slightly longer pulse than the one corresponding to Test 21 and it shows a higher specific energy efficiency.

Test Number 61

This was a rotating quartzite rock turning at 920 rpm. The radiation was 12.5 kw for 7 seconds. Again a spalled track was cut out with a volume of 3.580 cm^3. This represents a utilization 2.45 x 10^4 j/cm^3 amount of material removed. This figure is only slightly higher than for Test 60. The The principal difference between the appearance of this rock and that of Test 60 is that in the present case a crack was initiated through the entire 2.5 cm section of the rock and then propagated outward dividing the rock into three large pieces.

This data can also be analyzed as a succession of pulses. The duration is half that of Test 60; however, the specific energy consumption is just about the same. Therefore, the same remarks apply to the comparison between Tests 60 and 21.

Test Number 62

This was a basalt rock rotating 920 rpm, with a track 6.8 cm in diameter. The laser radiation was 12 kw for 6 seconds and the volume of material removed was .173 cm^3, giving an efficiency of 4.1 x 10^5 j/cm^3. This highlights the very large difference between basalt and quartzite once more. The low utilization of laser energy is probably due to the intense volume of smoke and the highly ionized plasma that is created with basalt.

Test Numbers 63 and 64

These were a pair of exposures on a granite block rotating at 460 rpm. The first exposure produced a ring 4.4 cm in diameter upon irradiation with 12 kw for 5.5 seconds. The volume that was removed was .51 cm^3 giving a utilization of 1.29 x 10^5 j/cm^3 of material removed.

The second exposure on this same rock produced a ring 6.8 cm in diameter. The laser radiation was 10 kw for 2.3 seconds. The volume that was removed was .216 cm^3 giving a utilization of 1.06 x 10^5 j/cm^3. There is close agreement between these two tracks in the granite although there was about 2.5 times difference in flux. This is in contrast to the track in basalt which used twice as much energy per cm^3 removed. This result is rather surprising because we have found in the penetration tests, that the interaction with granite requires more energy than with basalt.

In analyzing the data in Tests 62, 63 and 64 in terms of the succession of pulses there is considerably less consistency and also in the relative behavior of granite to basalt. We are of the opinion that the laser beam is partially absorbed by an ionizing plasma above rocks which contain sodium or potassium. It is very likely, that the amount of absorption and therefore the efficiency of the laser is quite variable from test to test depending on the particular mineral composition and the point being irradiated. The irradiated spot is a fraction of a millimeter in diameter whereas the rock grains themselves are somewhat larger.

The next group of experiments was done with the Avco Mark V laser located at our laboratory at Haverhill, Massachusetts, a few miles from the Everett Laboratory. This laser is a combustion driven laser; that is, the primary energy for producing the population inversion in CO_2 is derived from the combustion of fuel.[3] This laser has the capability to 20 kW, however when these particular exposures were run, the laser power varied from 15 to 17 kW as exhibited in the summary table of data, Table I. Also, the optics available with this laser was not of the same quality as used with our electrically pumped laser. Therefore, the spot size was larger than diffraction limited. For this reason, the experiments done with this laser were those in which we purposely wanted a larger spot size and a lower power density at the surface.

Test Numbers 225, 226 and 227

These three experiments used a rotating laser beam with a power of 14 kW directed in a circular path by a cam driven mirror. The path intersected three materials simultaneously, basalt, granite and quartzite, as shown in Fig. 8 which was taken during Experiment 227. In these experiments, the basalt and granite melted at the surface, however quartzite was spalled away with no visual evidence of melting. The three experiments differed in rate of revolution and spot size. The data, analyzed in Table II, is included in the general charts for rock removal. In the case of quartzite, the specific energy was of the order of 1.2 to 1.6 x 10^4 joules/cm^3.

Test Number 231

A sample of basalt was placed near the focal point of the F7 beam for a five second exposure to 15 kilowatts. From the motion picture taken during the exposure it was determined that 1.23 seconds was required for the beam to penetrate through 2.5 centimeters.

Test Number 232

Again a 14 kilowatt beam was directed onto the surface of basalt which was two inches inside the focal point of the F7 beam. The laser penetrated after 2.88 seconds, a depth of 2.2 centimeters.

D3433
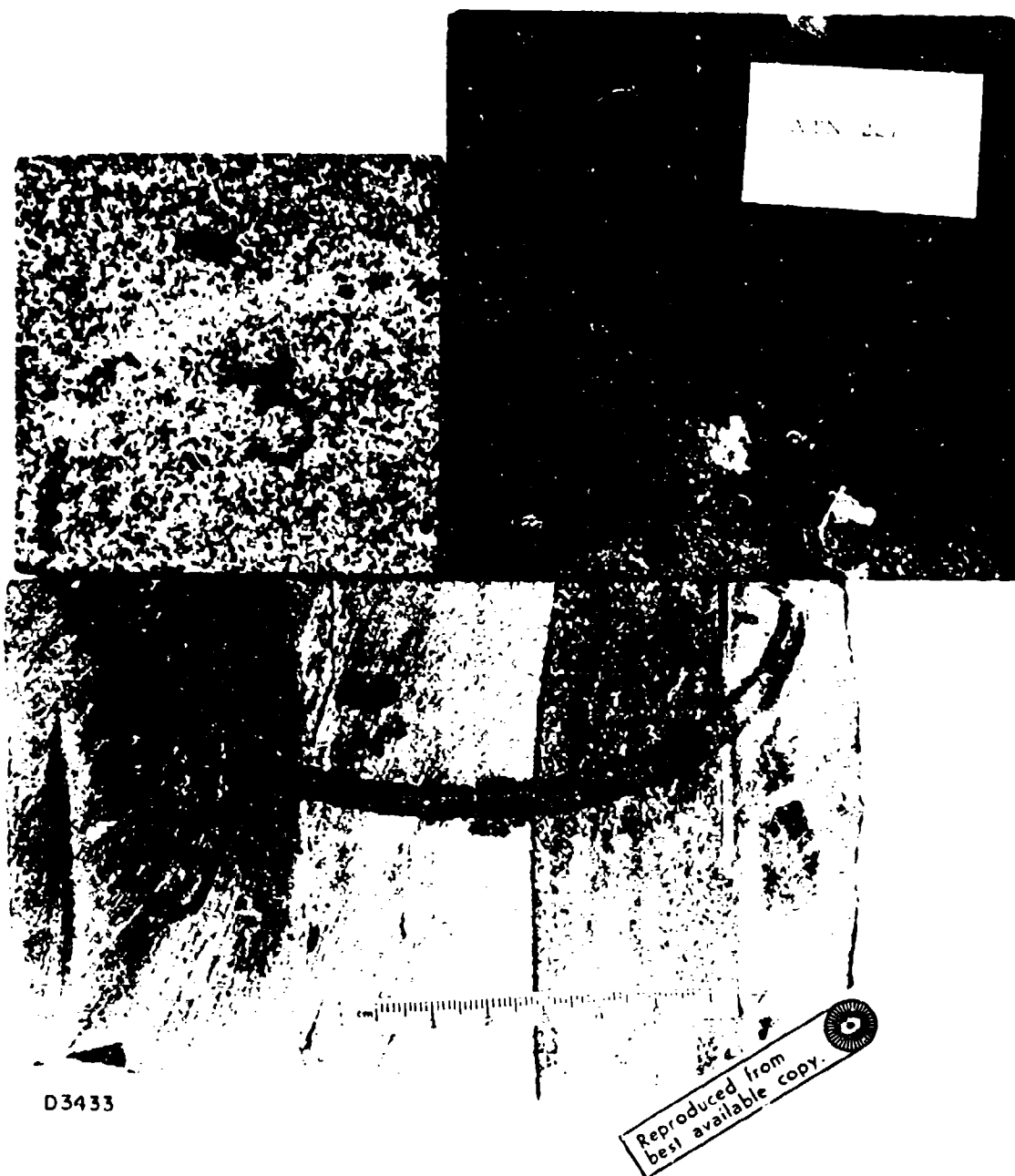
Figure 8 Exposure of three rocks simultaneously to a rotating beam
of 14 kW laser radiation. The larger rock is quartzite, at
the left is granite and at the right is basalt. The quartzite
was spalled. The other rocks were melted.

TABLE I

PENETRATION OF ROCKS BY CONTINUOUS WAVE LASER BEAM

Test No.	Rock Type	Laser Power $\left(\dfrac{watts}{\times 10^3}\right)$	Time (sec)	Laser Energy $\left(\dfrac{joule}{\times 10^3}\right)$	Spot Diam. (cm)	Peak Intensity $\left(\dfrac{watts}{cm^2}\right)$	Hole Depth (cm)	$\left(\dfrac{joules}{cm} \times 10^4\right)$
11	Q	11	2.1	23.1	.008	4.8×10^7	2.8	.82
12	Q	10.5	1.5	15.3	.008	4.6×10^7	2.3	.67
13	G	11	1.3	13.8	.008	4.8×10^7	2.5	.55
14	B	11	1.5	16.5	.008	4.8×10^7	2.5	.66
15	Q	11	3.9	43.0	.008	4.8×10^7	4.8	.90
16	B	10	1.5	15.0	.008	4.4×10^7	2.5	.60
1⟨	G	10	1.1	11.0	.008	4.4×10^7	2.5	.44
18	Q	11	2.5	27.5	.21	3.2×10^5	5.7	.48
19	G	11	2.33	25.6	.21	3.2×10^5	2.5	1.03
20	B	11	.83	9.1	.21	3.2×10^5	2.5	.36
51	B	1.25	2.7	3.4	.008	5.5×10^6	2.6	.13
52	G	1.25	11.2	14.0	.008	5.5×10^6	2.4	.59
53	B	5.1	1.3	6.4	.008	2.2×10^7	2.8	.23
54	Q	5.1	1.0	5.1	.008	2.2×10^7	1.9	.28
55	Q	5.1	2.0	10.2	.008	2.2×10^7	4.3	.24
56	Q	5.1⎫	4.0⎫		.008			
57	Q	10 ⎬	2.0⎭	30.4	.008		4.8	.64
58	G	1	6.0	6.0	.008	4.4×10^6	1.1	.54
59	G	10	.79	7.9	.008	4.4×10^6	2.5	.32
225	Q	14	1.69	23.66	.95	2.0×10^3	.49	.59
226	Q	13	2.02	26.26	.65	1.2×10^3	.26	.38
227	Q	14	1.58	22.12	.60	1.5×10^3	.24	.33
231	B	15	5.23	78.45	.538	6.6×10^4	2.5	.738
232	B	14	2.88	40.32	1.13	1.4×10^4	2.2	1.83
233	G	14	3.94	55.16	.538	6.2×10^4	2.7	2.04
234	Q	14.2	3.96	56.23	.61	4.9×10^4	2.65	.846

Test No.	Rock Type	Laser Power (watts $\times 10^3$)	Time (sec)	Laser Energy (joule $\times 10^3$)	Spot Diam. (cm)	Peak Intensity ($\frac{watts}{cm^2}$)	Hole Depth (cm)	($\frac{joules}{cm} \times 10^4$)
235	Q	14.1	7.15	100.82	.73	2.1×10^3	2.05	
236-239	Q	15.4	22.50	346.5	.95	1.1×10^3		
240-244	Q	16.3	20.00	326	.73	2.5×10^3		
245	Q	16	9.50	152	.73	2.4×10^3		
249	Q	15	.50	7.5	1.04	1.8×10^4	2.05	.366
253	Q	16.5	1.00	16.5	1.04	1.9×10^4		.825
254	B	17	1.00	17	.51	8.3×10^4		
255	B	16.5	.50	8.25	.51	8.1×10^4		.55
256	Q	17	.50	8.5	.85	3.0×10^4		.708
257	Q	17	.50	8.5	1.11	1.8×10^4		.81
1322	Q	.5	60.00	30	.363	2.1×10^2	.49	.32
1323	Q	1.0	180.0	180	.363	1.33×10^2	.575	.56
1324	Q	3.0	60.0	180	.363	4.2×10^2	1.15	.28
1327	B	15	20.00	300	.363	2.8×10^3	.621	1.06
1328	B	15	50.00	750	.363	1.4×10^3	.793	1.89
1663	Q	5	1.0	5	.008	2.2×10^7	3.48	.144
1664	Q	5	1.0	5	.008	2.2×10^7	3.10	.161
1665	Q	5.5	1.0	5.72	.008	2.4×10^7	3.33	.172
1666	Q	5	1.0	5.20	.008	2.2×10^7	3.60	.144
1667	Q	5	0.9	4.90	.008	2.2×10^7	3.42	.152
1668	Q	5	1.0	5.20	.008	2.2×10^7	3.33	.156
1669	Q	14.9	1.5	21.15	.008	6.6×10^7	3.72	.569
1671	Q	15	1.0	15.6	.008	6.6×10^7	4.72	.331
1672	Q	15	1.0	15.6	.008	6.6×10^7	4.63	.337
1673	Q	15	1.0	15.6	.008	6.6×10^7	5.00	.312
1674	Q	15.5	1.0	16.12	.008	6.8×10^7	4.95	.326
1675	B	5.5	1.3	7.15	.008	2.4×10^7	3.40	.210
1676	B	5.5	1.3	7.15	.008	2.4×10^7	3.50	.204
1677	B	5.5	1.0	5.72	.008	2.4×10^7	3.20	.179
1678	B	5.5	0.3	1.93	.008	2.4×10^7	1.90	.102

Test No.	Rock Type	Laser Power $\left(\frac{watts}{\times 10^3}\right)$	Time (sec)	Laser Energy $\left(\frac{joule}{\times 10^3}\right)$	Spot Diam. (cm)	Peak Intensity $\left(\frac{watts}{cm^2}\right)$	Hole Depth (cm)	$\left(\frac{joules}{cm} \times 10^4\right)$
1679	B	5.5	1.0	5.72	.008	2.4×10^7	2.50	.229
1680	B	5	1.0	5.2	.008	2.2×10^7	2.48	.210
1681	B	15	1.3	19.5	.008	6.6×10^7	4.63	.421
1682	B	15	1.3	19.5	.008	6.6×10^7	4.95	.394
1683	B	15	1.0	15.6	.008	6.6×10^7	4.70	.332
1684	B	15.25	1.0	15.86	.008	6.6×10^7	4.30	.369
1685	B	15.5	1.0	16.12	.008	6.8×10^7	3.73	.432
1686	B	15	1.0	15.6	.008	6.6×10^7	3.50	.446
1687	B	15.5	2.58	39.93	.008	6.8×10^7		
1708	Q	10.5	43.5	456.75	.008	4.6×10^7	13.85	3.298
1709	Q	5.5	40	220	.008	2.4×10^7	11.3	1.947

TABLE II

REMOVAL OF ROCK MATERIAL BY LASER BEAM

Test No.	Rock Type	Laser Power (10³ watts)	CW Exposure (sec)	Spot Size (cm)	Peak Intensity (w/cm²)	Material Removed (cm³)	CW Specific Energy (j/cm³)	Pulse Duration (10⁻³ sec)	Pulse Rep. Rate (sec⁻¹)
11	Q	11	2.1	.008	4.8×10^7	0.01		110	
11	Q	11	4.3	.008	4.8×10^7	0.86	5.5×10^4		
12	Q	11	1.5	.008	4.8×10^7	0.01	1.50×10^6		
15	Q	11	3.9	.008	4.8×10^7	0.04	1.20×10^6		
18	Q	11	2.5	.026	3.2×10^7	0.11	2.5×10^4		
21	Q	11	1.9	.008	4.8×10^7	0.43	4.8×10^4	2.4	6.7
23	B	11	2.1	.008	4.8×10^7	0.12	1.9×10^5	8.4	6.7
24	G	11	2.1	.008	4.8×10^7	0.24	9.8×10^4	11.	6.7
22	Q	11	2.5	0.21	3.2×10^5	0.95	2.9×10^4	30.	6.7
32	Q	11.5	3.8	3.10	1.5×10^3	4.44	9.7×10^3	420.	
33	Q	11.5	3.7	6.30	3.7×10^2	6.14	6.9×10^3	750.	
34	Q	11.5	3.6	1.50	6.5×10^3	4.74	8.9×10^3	267.	
31	B	11.5	4.5	.008	5.1×10^7	0.15	1.1×10^5	50.	
35	B	11.5	5.3	1.40	7.5×10^3	1.53	4.0×10^4	470.	
36	B	11.5	5.5	3.10	1.5×10^3	1.17	3.2×10^4	780.	
37	G	11.5	4.3	3.10	1.5×10^3	1.01	4.8×10^4	630.	
38	G	11.5	4.1	1.05	1.4×10^4	0.74	6.3×10^4	340.	
51	B	1.3	9.3	.008	5.7×10^6	0.10	1.0×10^5		
52	G	1.3	12.9	.008	5.7×10^6	0.06	2.3×10^5		
53	B	5.1	2.5	.008	2.2×10^7				

Test No.	Rock Type	Laser Power (10³ watts)	CW Exposure (sec)	Spot Size (cm)	Peak Intensity (w/cm²)	Material Removed (cm³)	CW Specific Energy (j/cm³)	Pulse Duration (10⁻³ sec)	Pulse Rep. Rate (sec⁻¹)
54	Q	5.1	1.0	.008	2.2×10^7	0.01	8.2×10^5		
55	Q	5.1	2.0	.008	2.2×10^7	0.02	6.6×10^5		
60	Q	10.8	6.5	.008	4.8×10^7	3.71	1.8×10^4	7.9	7.7
61	Q	12.5	7.0	.008	5.5×10^7	3.58	2.5×10^4	4.1	15.3
62	B	12	6.0	.008	5.3×10^7	0.17	4.1×10^5	2.1	15.3
63	G	12	5.5	.008	5.3×10^7	0.51	1.3×10^5	3.3	7.7
64	G	10	2.3	.008	4.4×10^7	0.22	1.1×10^5	1.3	7.7
225	Q	14	1.7	0.95	2.0×10^4	1.88	1.3×10^4	7.2	8.3
226	Q	13	2.0	0.65	3.9×10^4	1.60	1.6×10^4	1.8	11.3
227	Q	14	1.6	0.60	4.9×10^4	1.43	1.5×10^4	1.0	18.3
231	B	15	5.2	0.54	6.6×10^4	1.56	5.0×10^4		
232	B	14	2.9	1.13	1.4×10^4	1.32	3.1×10^4		
233	G	14	3.9	0.54	6.2×10^4	0.58	9.5×10^4		
234	Q	14.2	4.0	0.61	4.9×10^4	0.64	8.8×10^4		
235	Q	14.1	7.2	0.73	2.1×10^4	3.92	2.6×10^4	5.5	16.7
236-238	Q	15.4	22.5	0.95	1.1×10^4	24.60	1.4×10^4	3.6	16.7
240-244	Q	16.3	20.0	0.73	2.5×10^4	27.70	1.2×10^4	5.0	18.3
245	Q	16	9.5	0.73	2.4×10^4	17.80	8.5×10^3	5.0	18.3
249	Q	15	0.50	1.04	1.8×10^4	0.33	2.3×10^4		
253	Q	16.5	1.0	1.04	1.9×10^4	0.52	3.2×10^4		
254	B	17	1.0	0.51	8.3×10^4	0.27	6.3×10^4		
255	B	16.5	0.5	0.51	8.1×10^4	0.12	6.9×10^4		

Test No.	Rock Type	Laser Power (10³ watts)	CW Exposure (sec)	Spot Size (cm)	Peak Intensity (w/cm²)	Material Removed (cm³)	CW Specific Energy (j/cm³)	Pulse Duration (10⁻³ sec)	Pulse Rep. Rate (sec⁻¹)
256	Q	17	0.5	0.85	3.0×10^4	0.35	2.4×10^4		
257	Q	17	0.5	1.11	1.7×10^4	0.53	1.6×10^4		
1322	Q	0.5	60.	0.36	6.6×10^2	1.80	1.7×10^4	2.1	21.7
1323	Q	1.0	180.	0.36	1.3×10^3	10.00	1.8×10^4	1.4	12.5
1324	Q	3.0	60.	0.36	4.2×10^3	18.20	9.9×10^3	1.4	12.5
1327	B	15	20.	0.36	1.4×10^5	13.94	2.1×10^4	1.4	15.
1328	B	15	50	0.36	1.4×10^5	39.55	1.9×10^4	1.1	10.7
1663	Q	5	1.0	.008	2.2×10^7	0.029	1.7×10^5	CW	
1664	Q	5	1.0	.008	2.2×10^7	0.026	1.9×10^5	CW	
1665	Q	5.5	1.c	.008	2.2×10^7	0.028	2.0×10^5	12.	13.3
1666	Q	5.	1.0	.008	2.2×10^7	0.031	1.7×10^5	12	
1667	Q	5.	0.9	.008	2.2×10^7	0.029	1.6×10^5	1	156.7
1668	Q	5.	1.0	.008	2.2×10^7	0.028	1.8×10^5	1.	156.7
1669	Q	14.9	1.5	.008	6.6×10^7	0.153	1.4×10^5	CW	
1670	Q	14.9	1.5	.008	6.6×10^7	0.030	7.1×10^5	CW	
1671	Q	15	1.0	.008	6.6×10^7	0.195	8.0×10^4	12	13.3
1672	Q	15	1.0	.008	6.6×10^7	0.191	8.1×10^4	12	13.3
1673	Q	15	1.0	.008	6.6×10^7	0.206	7.6×10^4	1	156.7
1674	Q	15.5	1.0	.008	6.8×10^7	0.204	7.9×10^4	1	156.7
1675	B	5.5	1.3	.008	2.4×10^7	0.21	3.4×10^4	CW	
1676	B	5.5	1.3	.008	2.4×10^7	0.30	2.3×10^4	CW	
1677	B	5.5	1.0	.008	2.4×10^7	0.18	3.1×10^4	12	13.3

Test No.	Rock Type	Laser Power (10³ watts)	CW Exposure (sec)	Spot Size (cm)	Peak Intensity (w/cm²)	Material Removed (cm³)	CW Specific Energy (j/cm³)	Pulse Duration (10⁻³ sec)	Pulse Rep. Rate (sec⁻¹)
1678	B	5.5	0.3	.008	2.4×10^7	0.03	4.8×10^4	12	13.3
1679	B	5.5	1.0	.008	2.4×10^7	0.11	5.2×10^4	1	156.7
1680	B	5	1.0	.008	2.2×10^7	0.12	4.3×10^4	1	156.7
1681	B	15	1.3	.008	6.6×10^7	0.20	9.8×10^4	CW	
1682	B	15	1.3	.008	6.6×10^7	0.41	4.8×10^4	CW	
1683	B	15	1.0	.008	6.6×10^7	0.21	7.4×10^4	12	13.3
1684	B	15.5	1.0	.008	6.8×10^7	0.42	3.8×10^4	12	13.3
1685	B	15.5	1.0	.008	6.8×10^7	0.44	3.7×10^4	1	156.7
1686	B	15	1.0	.008	6.6×10^7	0.56	2.8×10^4	1	156.7
1687	B	15.5	2.5	.008	6.8×10^7			12	13.3
1708	Q	10.5	43.5	.008	4.6×10^7			CW	
1709	Q	5.5	40	.008	2.4×10^7			CW	
1710	Q	10	90	.10	3.1×10^3	120.	7.5×10^3		
1711	Q	5	100	.10	1.5×10^3	28	1.8×10^4		
1712	B	5.25	270	.10	1.6×10^3	11	1.3×10^5		

Test Number 233

The 14 kilowatt laser beam was directed to the face of granite which was placed near the focal point of the beam. The penetration time was 3.94 seconds for a 2.7 centimeter depth.

Test Number 234

A quartzite rock was placed near the focal point of the F7 beam with 14 kilowatts of power. The burn through time was 1.58 seconds and the penetration was 2.65 centimeters.

Test Number 235

A larger block of quartzite was placed near the focal point of the F7 beam and the beam was directed in a circular pattern of one inch in diameter at a rate of 1000 rpm. The exposure time was 7 1/2 seconds. A total of 3.92 cm^3 of material was removed with power density of 2.1 kilowatts per cm^2, resulting in a specific energy removal rate of 2.57×10^4 j/cm^3. The rock is illustrated in Fig. 9.

Test Numbers 236, 237, 238 and 239

A 16 kilowatt laser was directed in a 5 cm circle for four repeated experiments. The total time of exposure was 22 1/2 seconds. The total amount of material removed was 24.6 cm^2 with an intensity approximately 1 kW/cm^2. The specific energy required was 1.4×10^4 j/cm^3.

Test Numbers 240, 241, 243 and 244

The beam was directed onto quartzite in a 5 cm circle at 1100 rpm. Shorter exposures were now used at approximately four seconds each for a total of 20 seconds exposure. At the end of each exposure material which had accumulated in the hole in the quartzite was brushed out. A total of 27.7 cm^3 of material was removed with a specific energy of 1.18×10^4 j/cm^3.
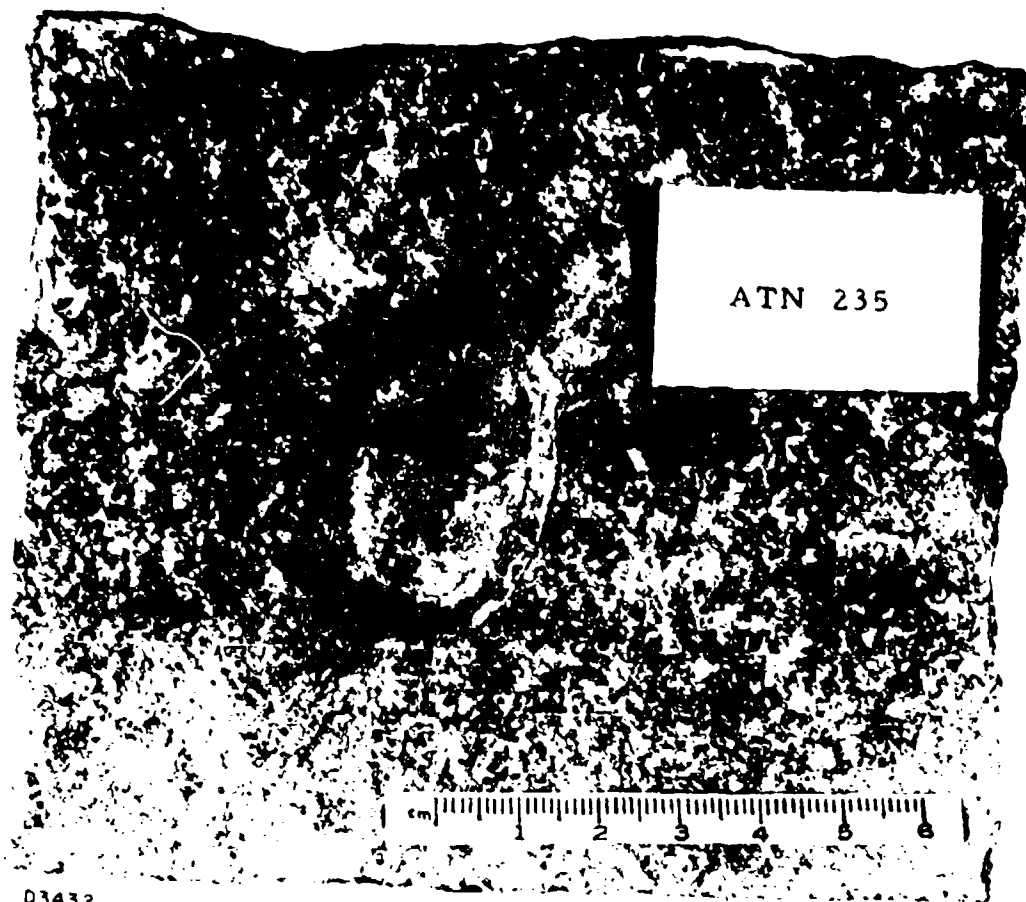
Figure 9   Exposure of a block of quartzite to 14 kW laser radiation for 7.5 seconds.   The beam was rotated at 1000 rpm.   See the test for Experiment No. 235.

Test Number 245

For this experiment, which is a repeat of the above, high pressure nitrogen was directed onto the face of the rock where the laser beam was interacting. The purpose of this was to clear the material out as it formed. A 16 kilowatt beam was directed for 9 1/2 seconds onto the face of the rock. A total of 17.8 cm^3 was removed. The specific energy for this test was 8.54×10^3 j/cm^3 (see Fig. 10).

Test Numbers 249, 253, 254, 255, 256, 257 and 258

Both quartzite and basalt were run at approximately 20 kilowatts near the focal point of an F7 beam. The beam was not diffraction limited and in fact the effective diameter was many times the diffraction limit. These experiments are tabulated in Table II.

The same experiments could be interpreted in terms of a pulsed laser beam since each spot on the rock face received a succession of pulses equal to the transit time of the beam over the spot.

The next set of experiments were done with an electrically pumped laser reaching up to 15 kilowatts. The beam was always focused on the surface. Three types of exposure were done namely continuous, pulsed and rotating beam. The rotating beam was generated by a cam operated mirror. Pulses were obtained by placing a rotating chopper wheel in the path of the beam. This wheel contained two apertures giving a duty cycle of 16%.

Test Numbers 1663 and 1664

These were one second CW exposures of quartzite at 5000 watts power. The first was without the gas jet; the second with it. Penetration for the first was 3.48 cm; the second 3.10 cm for 5000 joules of energy.

Test Numbers 1665 and 1666

These were 6.5 second elapsed time exposures of quartzite at approximately 5000 watts power with the chopper rotating at 400 rpm,
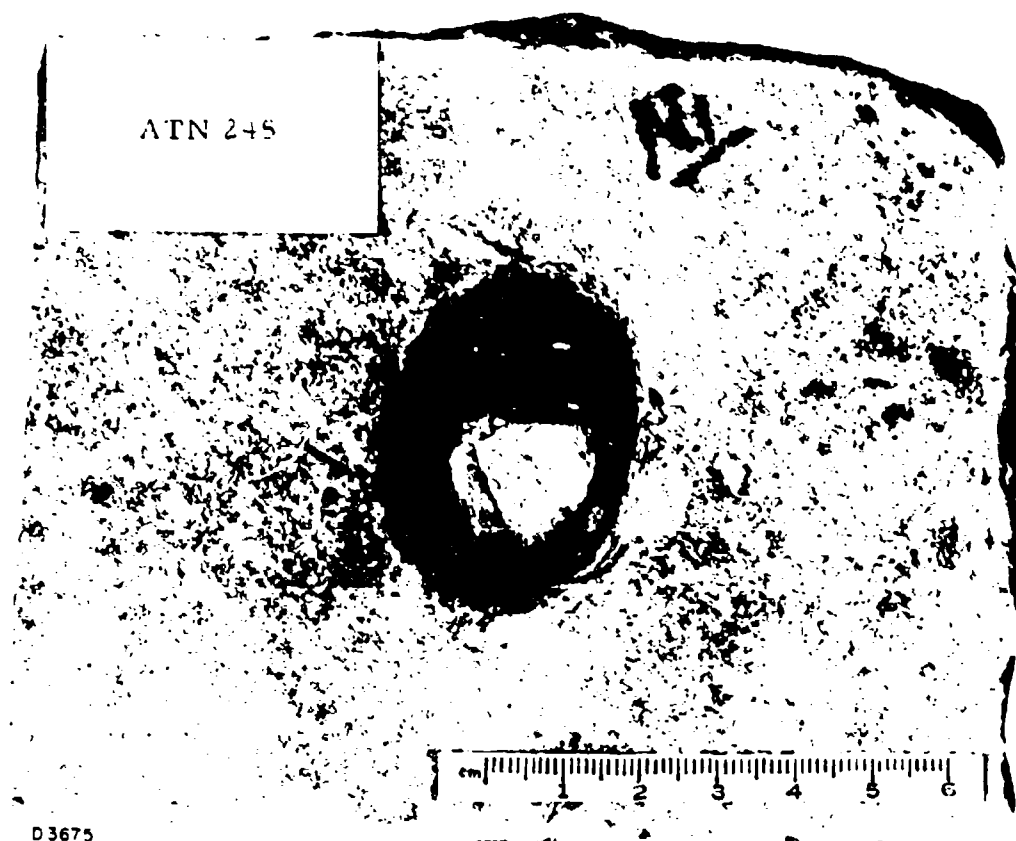
Figure 10   In this experiment, Number 245 a quartzite block was
             exposed to a 16 kW laser beam for 9.5 seconds. The
             beam was rotated on the face and the loose material
             was blown away by a nitrogen jet.

13. 3 pulses per second with a duration of 12 milliseconds. That is, the
rock was actually exposed for 16% of this time. Penetration for Test
Number 1665 was 3.33 cm for 5720 joules (w/o gas jet); for 1666 - 3.60 cm
for 5200 joules (with gas jet).

Test Numbers 1667 through 1674

Experiment Number 1667 and 1668 were exposures of quartzite at
5 kilowatts with a 1 millisecond pulse and an elapsed time of 6.5 seconds.
Number 1667 was without nitrogen gas and 1668 had a gas jet. In the case
of 1667, the laser was mistakenly shut off before the 6.5 seconds exposure
had ended. The actual exposure of 6.1 seconds was gotten from the movie
film. Penetration was 3.42 cm for 4900 j. In the case of 1668, penetration
was 3.33 cm for 5200 j. Thus, the gas jet did not assist the rate of drilling.
This is because the drill hole is filled with rock vapor and ionized plasma
which is flowing out with a velocity sufficiently high to interfere with the
penetration of the gas jet. In the case of Experiments 1669 to 1674, laser
power was 15 kW and again three types of exposures were used. 1669 and
1670 were continuous exposures for one second. 1671 and 1672 were 6 1/2
seconds of exposure at 12 milliseconds but the total time was one second.
1673 and 1674 were 6 1/2 seconds exposures to one millisecond pulses. The
data is given in Table I and the results are included in the general map of
penetration data. The observations here show that the rate of penetration
is very slightly different among the different experiments, within the expected
scattering. Thus we would conclude that down to one millisecond pulses, the
rate of penetration is a function of energy and not of pulse width. Data for
Experiment 1670 is not included in the table because through some discre-
pancy, it was not possible to probe the depth of the hole. A conclusion from
this test, done with quartzite, is that the laser is just about twice as effi-
cient in using power to drill a hole with 5 kilowatts as compared to 15 kilo-
watts.

Test Numbers 1675 through 1686

This is a group of twelve experiments done with basalt and was
identical to the preceding set of twelve done with quartzite. Again, CW

exposures of one second were used, and pulsed exposures of twelve and one millisecond were used with a total exposure time of 6.5 seconds and a rock exposure of one second. The same group was repeated with both 5 kilowatts and 15 kilowatts laser power. The results are entered in Table I for the general summary of the rock penetration experiments and on the general map. Again the same conclusions as in the case of quartzite follow; namely that the rate of penetration is proportional to the kilojoules of exposure, but not dependent on the pulse width. The penetration with 15 kilowatts laser power was only twice that when 5 kilowatts was used, other conditions being equal. This is very similar to the results obtained with quartzite. In this series of exposures, each experiment was repeated twice, once with gas and once without gas. No dependence was observed of the depth of penetration on gas assist. There was one experiment, namely 1678 where the laser was shut off after 2.2 seconds instead of 6.5 seconds. This gave a hole which was not as deep as for the 6.5 seconds but enabled us to determine whether or not the efficiency of penetration was a function of hole depth. In Test 1677, about 1800 j/cm of penetration is required and in Experiment 1678, only 1000 j/cm is used.

Test Numbers 1708 and 1709

These two experiments were deep penetrations in a six inch block of quartzite. These tests are illustrated in Fig. 11. In Experiment 1708, the laser power was 10.5 kilowatts and penetration occurred with 457 kilojoules for 13.9 cm. In Experiment Number 1709, the laser power was 5.5 kilowatts and penetration occurred with 220 kilojoules for 11.3 cm. These experiments are noteworthy in that they show that for deep penetration, the laser efficiency is very low. Comparing Experiment 1709 where a 5 kilowatt laser penetrated 11 cm and Experiment 1663 where the same laser penetrate 3.5 cm, shows a penetration energy per cm of more than an order of magnitude lower for the shorter depth. We have analyzed the way in which the laser interacts with the products of vaporization in a hole in connection with other work at this laboratory. The analysis shows that there is a very strong absorption of laser radiation in the gases within the hole. Theoretically, there is an asymptotic limit to the depth of penetration for any laser power. This theory is consistent with the present experimental observations.

Figure 11 Penetration of six inch thick rocks of quartzite by a laser beam. The one at the left was with 5.5 kilowatts. The one on the right was 10.5 kilowatts. The lower power laser penetrated with about 65% of the energy as the higher power laser.

The next group of experiments deal with an attempt to spall the center out of large blocks of rock using a rotating laser beam. Two types of rocks were used quartzite and basalt. The range of laser power was from 500 watts to 15 kilowatts. The circle of radiation was up to six inches diameter. The general results are contained in the table for rock removal and plotted on the general maps. More specifically:

Test Numbers 1322 through 1328

The first four exposures were in quartzite. This is illustrated in Fig. 12. The results in quartzite are similar to what we have already observed in other experiments, namely, that the larger spot has a higher efficiency for rock removal and that, since the surface intensity is quite low, the laser energy does not play a significant role.

Test Numbers 1327 and 1328

These are exposures in basalt with 15 kilowatts with a two inch and four inch circle respectively. This experiment is illustrated in Fig. 13. In this photograph, one sees that basalt was spalled in a similar way to quartzite. The spalled out section was placed on top of the rock when it was subsequently photographed. The results of these experiments are included in Table II.

Test Numbers 1710, 1711 and 1712

These were exposures of quartzite and basalt blocks to an even larger circle, namely six inches diameter and lower powers namely 5 and 10 kilowatts. Test Number 1710 was an exposure of quartzite to 10 kilowatts, 1711 was quartzite at 5 kilowatts and 1712 was basalt at 5.25 kilowatts. The results are given in Table II. In the case of quartzite, the rock was easily spalled giving specific energies for rock removal consistent with the preceding experiments for large circular tracks in quartzite. The case of basalt, at low power and very long time of exposure, the heat was diffused in the block. We did not get spalling under these conditions. Instead there was some vaporization at the surface and the specific energy for rock removal is high, about an order of magnitude higher than for quartzite.

Figure 12 A 13 inch square block of quartzite exposed to rotating laser beams with power from .5 to 3 kilowatts.

-50-

D3435

Figure 13   A one foot square block of basalt exposed to rotating laser
beam of 15 kilowatts power. This produces spalls in the
basalt, similar to that in quartzite.

The next three experiments to be described were exposures of quartzite blocks to extremely short duration pulses using a short pulsed laser.

Test Numbers 2-8-72-3, 2-8-72-4

These two exposures were with 1125 j and 900 j for 20 μ secs and 17 μ secs respectively. A diffraction grating was used in the first experiment so that an estimate of the energy in the zero order focal point could be made from measuring the power in the fifth order. The grating was not used after the first exposure. In these experiments, there were numerous breakdowns in the air in front of the sample. These were initated by dust particles in the air and as a consequence very little is known about the actual energy that was received by the rock. Figure 14 shows a photograph of the air breakdown.

Test Number 2-8-72-5

In this experiment, a quartzite block was used with the hole predrilled approximately 1/2 inch diameter and one inch deep. The rock was placed sufficiently ahead of the breakdown region so that the laser could illuminate the bottom of the hole. The exposed area was approximately 2 cm by 4 cm. With a total exposure of 500 joules in 10 μ secs.

In the above experiments there was no visible effect on the rock.
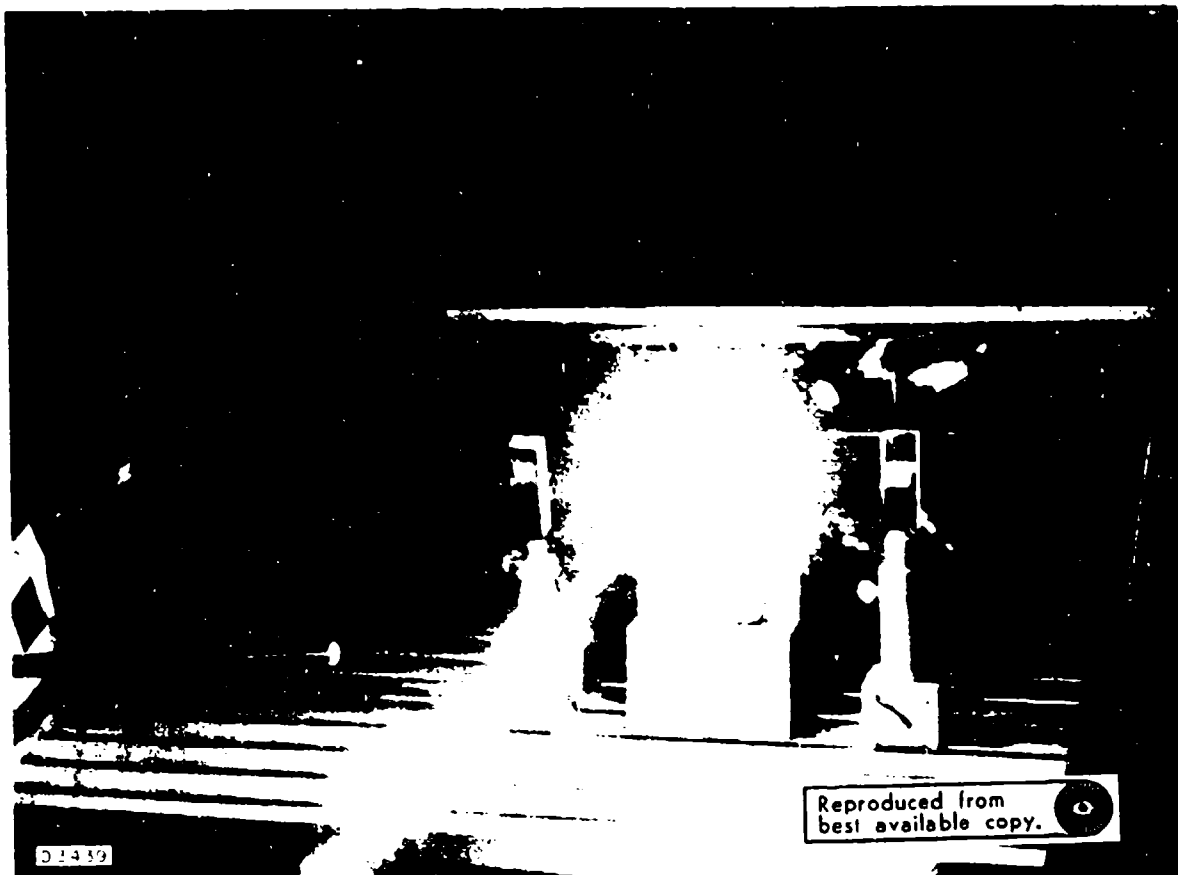
Figure 14   A block of quartzite exposed to about 1000 j of laser power in
20 microseconds.   The intensity was sufficient to break down
the air ahead of the sample, thus shielding the rock from the
laser energy.

IV. CONCLUSIONS FROM ROCK PENETRATION TESTS

Penetration of Rocks

The penetration of quartzite, basalt and granite was obtained from the experiments described in Section III. The data is presented in Table I which shows the depth of a hole drilled by the laser as a function of power, rock type and spot size. The symbol under material, Q, G, B identify quartzite, granite and basalt respectively. For the spot diameter, the sharply focused spots were taken as .008 cm according to the arguments presented in Section II. For defocused spots, the spot diameter was obtained from geometrical optics considerations. For annular type of laser beams as used in this laboratory, we have already stated that 22% of the total laser energy is contained within a .008 cm spot diameter. In this way, the peak intensity was evaluated. The remainder forms a more diffused pattern as a result of diffraction. The penetration depth was obtained by probing or by timing the passage of the laser beam through the rock with motion pictures taken during the exposure.

Figure 15 presents a portion of the penetration data in graphical form. The type of rock is identified by the symbol. All of the data points for sharply focused beams and for 2.21 cm diameter spots are shown and distinguished by the type of symbol. This data suggests that a laser of about 5 kilowatts power is more efficient in penetration than one of higher power.

All of the data of Table I is again plotted in Figure 16 with laser intensity in watts/cm^2 as the independent variable. This covers about six orders of magnitude in laser intensity and shows that the penetration energy varies only about one order of magnitude over this entire range. There is a considerable amount of scattering which is due to the nature of the rocks and the type of experiment. The minimum corresponding to 5 kilowatts of laser power appear on this figure around the 2.5×10^7 w/cm^2 abscissa.
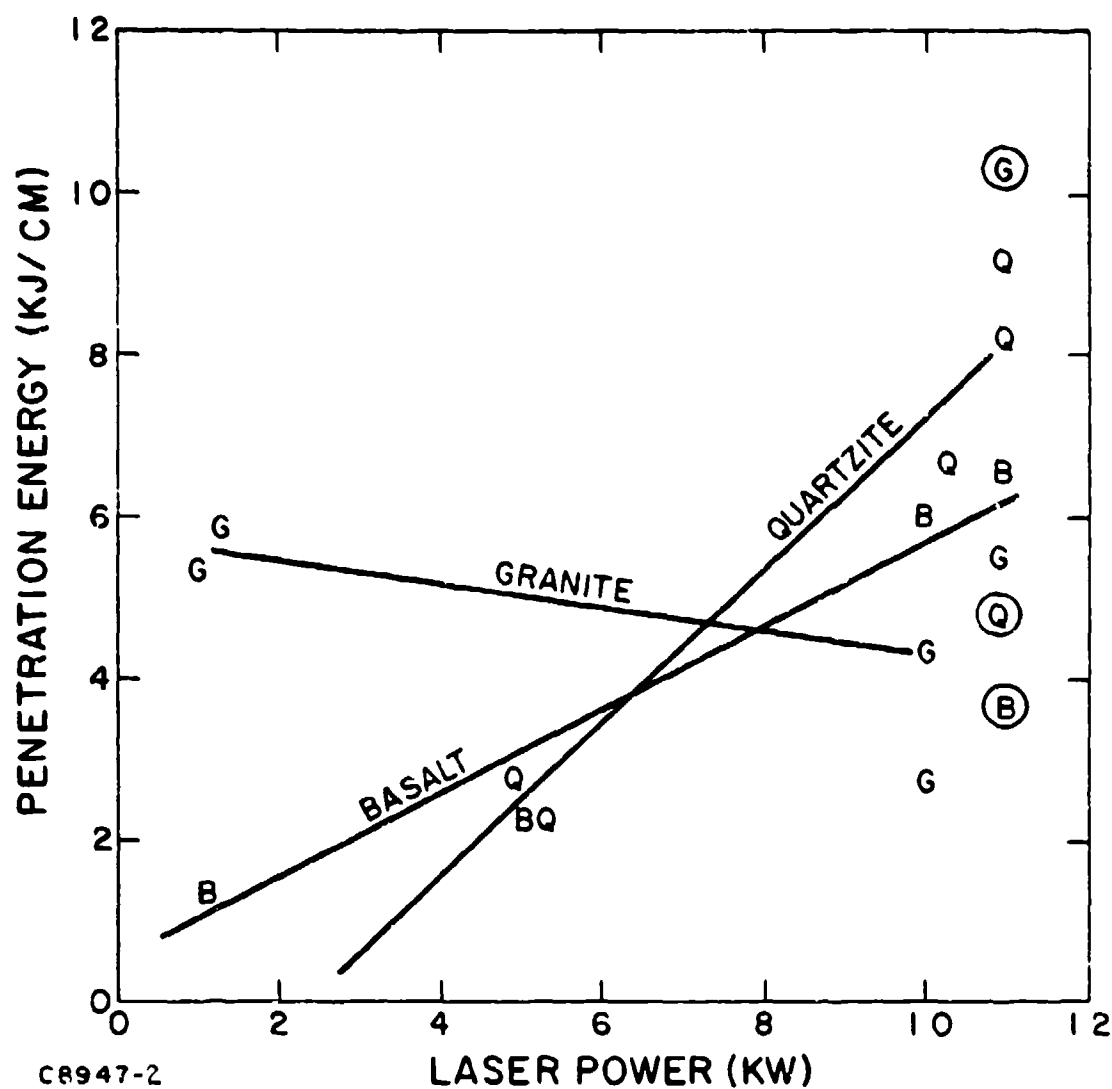
Preceding page blank

Figure 15   Energy required to penetrate rocks. The symbols identify
quartzite, basalt, and granite. The symbols enclosed in
circles are for 2 mm spot diameter. The other symbols
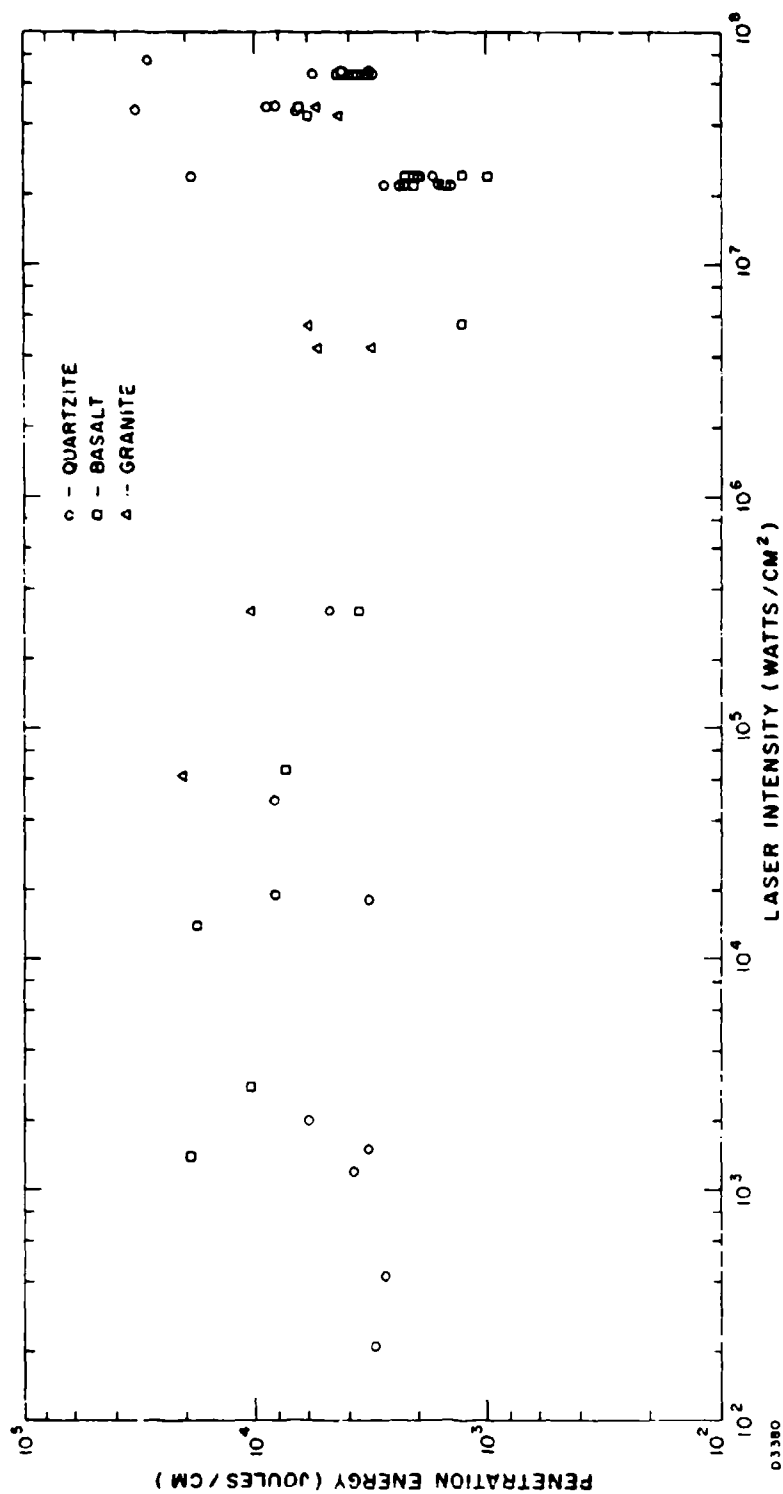are for sharply focussed spots.

Figure 16   A general map of the energy required to penetrate rocks plotted against C. W. laser incident intensity. Six orders of magnitude of intensity are represented.

-57-

Rock Removal by the Laser

Rock removal was accomplished in by both vaporization, and by spalling. Different types of hard rocks were used, different spot sizes, and different intensities. All of the rock removal data is given in Table II. This data is also plotted in Figure 17. It has already been mentioned in the preceding section that rock removal was not a function of pulse duration for pulses from 1 millisecond up to CW. This figure shows scattering in the data but this is not surprising since the one figure combines very different types of tests, vaporization tests as well as spalling tests. All of the tests below about 10^4 watts/cm^2 are for rock removal by spalling and the tests above 10^5 watts/cm^2 represent vaporization. Also represented on this curve are a variety of spot sizes, a difference in the laser power and the type of rock. What this figure shows is that there is only a slight dependence of specific energy on laser intensity. While the intensity varies by six orders of magnitude, the specific energy for rock removal varies by only about one order. The solid line in this figure is drawn with a slope that represents a fifth root dependence of the specific energy on intensity.

Another significant thing about this figure is that whatever small advantage there is lies with lower spot intensities, provided the intensity is high enough to remove rock at all.

In other work at this laboratory, we have developed a theory of the interaction of a laser beam with rock materials being vaporized. The vapor fills a hole through which the beam is transmitted. This analysis which takes into account the viscosity of the out flowing gases and the absorption of laser beam energy due to the free electron intensity. The conclusion of this work is that there is an asymptotic limit to the depth of penetration by a laser beam. This limit is only weakly dependent on the incident laser intensity. A small diameter hole quickly reaches a maximum penetration of a few cm then grows slowly in depth and diameter resulting in inefficient use of laser radiant power. These theoretical results are consistent with experiments.
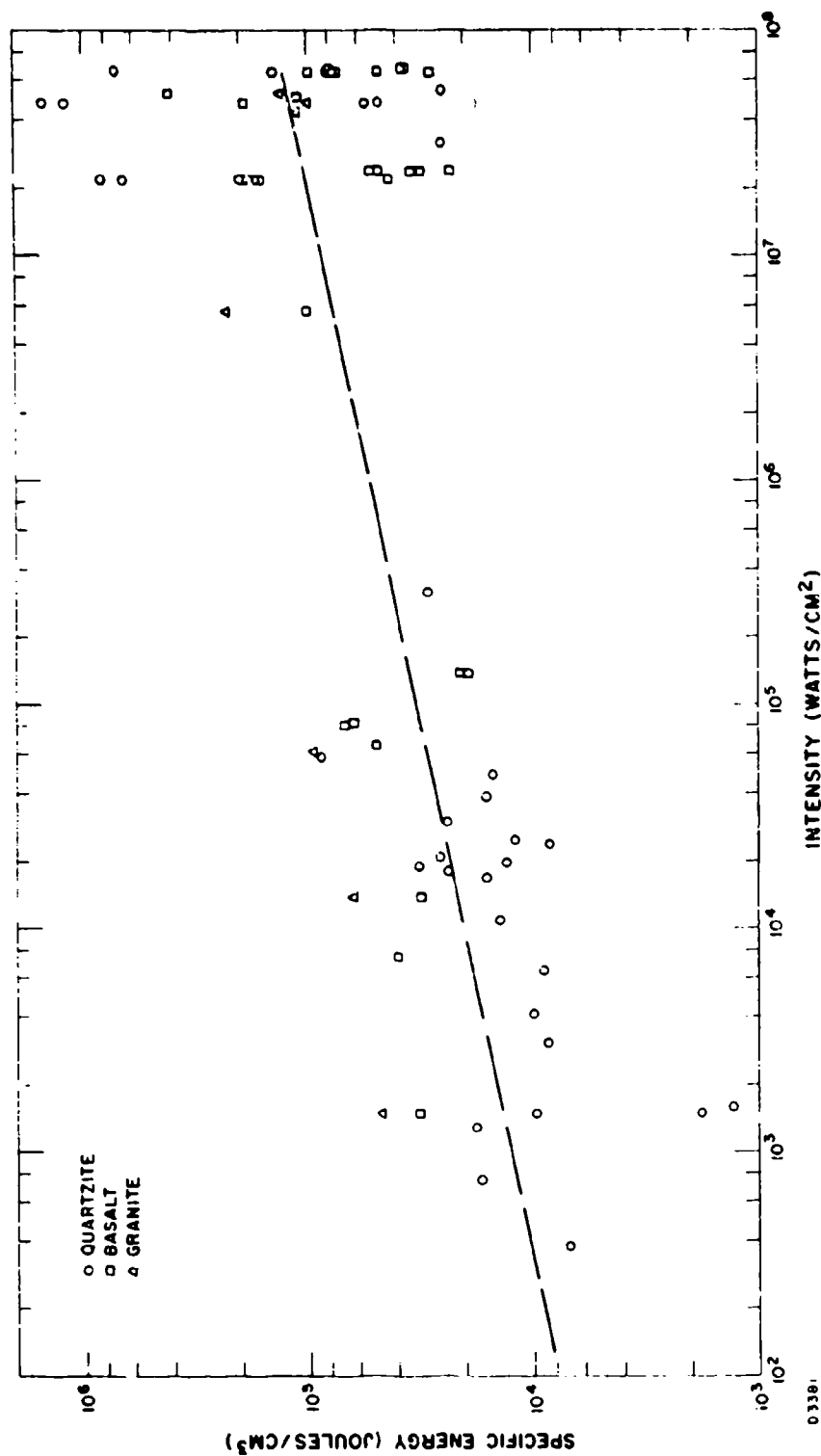
-58-

Figure 17 A general map of the specific energy required to remove rocks plotted against laser spot intensity. Represented here are vaporization as well as rock spalling, various spot sizes, laser power, and rock types. The specific energy varies with the fifth root of the laser intensity.

V. MECHANICAL STRESS FROM SHORT LASER PULSES

In this section we will analyze theoretically the type of interactions that might result from microsecond length laser pulses. The laser intensity may be large enough to reach the limit of transmission through the atmosphere and we would like to know whether in such a case, sufficiently powerful elastic waves can be generated to crack large rocks.

Two types of interactions are considered. The first is the heating of the surface. The second is a direct pressure pulse. Temperature diffuses into the material as the square root of the time.

$$d = \sqrt{\frac{kt}{\rho \bar{C}}} \tag{1}$$

Here k is the thermal conductivity (approximately 1.2 w/m $^\circ$K for hot granite); t is the pulse time; ρ is the density (2700 kg/m^3); and $\bar{C}$ is the average specific heat (approximately 800 j/kg $^\circ$K). The heat penetrates a distance of 0.007 mm during a 100 microsecond pulse. We will see that the radius to be irradiated is about 100 times this distance, so that during the pulse, only a very thin skin has been heated. This means that the surface will not expand very much because of constraint by the material below the heated spot. Nevertheless, just to prove the point, in the part that follows, we will allow the heated zone to expand with the same expansion coefficient, α, as for a uniformly heated body. This will lead to a larger value of stress than we can actually expect.

The boundary of the heated zone will then have a strain

$$\epsilon = \alpha T \tag{2}$$

Preceding page blank

where $\alpha = 1.5 \times 10^{-5}$ per $^\circ C$ for granite where T is the temperature (limited to $2500^\circ K$ or else we will waste laser energy in ablation). The heated zone will move with a velocity

$$v = \frac{r\epsilon}{t} = \frac{\alpha r T}{t} \tag{3}$$

The stress resulting from this velocity is

$$\sigma = \rho c v \tag{4}$$

where

$$c = \sqrt{\frac{E}{\rho} \; \frac{1 - \nu}{(1 + \nu)(1 - 2\nu)}} \approx \sqrt{\frac{E}{\rho}}$$

(This expression is easily derived if one considers that the expanding heated zone transfers momentum to the surrounding material at the rate of ρc per unit area.)

The maximum incident laser power that can be used

$$P = \frac{\rho C T}{t} \; \pi r^2 \sqrt{\frac{kt}{\rho C}} = \pi T r^2 \sqrt{\frac{k \rho C}{t}} \tag{5}$$

$$r = \frac{\sigma t}{\alpha T \sqrt{E \rho}} \tag{6}$$

The heated spot is expanding. It generates a pressure pulse traveling radially outward, followed by a tension pulse immediately behind. The strain near the surface is tangential to the heated zone, and if a crack were to result it would be a circular one surrounding the laser spot. At distances from the source, the intensity of the wave decays as $1/r^2$ or faster. Near the source,

we can use Equations (5) and (6) to determine the maximum useful power consistent with a 2500°C failure stress of 1200 psi ($\sigma = 8.2 \times 10^6$ n/m^2).

From Equation (6) we find r = 0.2 cm and the incident power is 4400 watts (0.4 joule).

Actually, because the heated zone is so thin, it will expand at a much lower rate with a lower stress. Underneath the heated zone, the material is expanding in a direction parallel to the surface, leading to a shear that is resolved at 45 degrees into a tensile stress that tends to split off the heated material as a flake. This is exactly what was observed when we irradiated quartzite with 1 joule pulses in the experiment described under Section III's, Pulsed Experiments. We found small spalls, that is, shallow depressions in the surface.

This brings up the second way in which a powerful pulsed laser can interact. As a result of the ablation pressure, the surface can be driven inward with a pressure of the order of 100 atmospheres. At the boundary of the pressure region, that is, in or near the surface, there is a shear wave that is not strong enough to cause the rock to fail. If this moves off any appreciable distance from the source, its intensity decreases as $1/r^2$ and so it is not effective. Beneath the pressure pulse, the wave is a longitudinal compression pulse not strong enough to cause failure unless it is reflected from a free surface. Again, because of the $1/r^2$ dependence, this must occur within a few spot diameters of the source to have a large effect. Thus, it is conceivable that a pressure pulse can split off the back of a thin plate.

The conclusion of this simple theory is that a pulsed laser is not likely to crack large rocks by any simple interaction. It is conceivable that individual pulses can be combined by interference to produce intensification of the stress.

VI. COMPUTER PROGRAMS FOR THERMO-ELASTIC STRESS ANALYSIS

In order to study how thermal stress is created and propagated in rocks we have developed two computer programs which use the finite element method for computing temperature distributions, stress and strain distributions, throughout a body. These particular programs are quite general in that they can accept any heat flux, and temperature distribution whether from a point source, an annulus, generated on the surface, or in the interior of a body. Certain parts of the body can be held at fixed temperatures. A nonlinear thermal conductivity coefficient is used containing two adjustable parameters. Mechanical forces or boundary conditions can be superimposed on the thermal ones. Also, the elastic properties may be different in different directions and may also be a function of temperature. Finally, since temperatures at the surface may get above the boiling point, the program has an adjustable cutoff so that temperatures above the boiling point are not permitted.

There are actually three computer programs. The first one, called ROAST is based on a program obtained from Professor McGarry of M. I. T. except that it is modified to allow nonlinear thermal conductivity. Our program also contains procedures which iterate in small time steps to arrive at the temperature of an element. Otherwise, the very sudden increase in temperature resulting from high intensity laser radiation actually causes an instability in the computer program which obviously does not occur in practice. The output of the program ROAST is a distribution of temperature in the radial and depth directions in the body as a function of time. These temperatures may be plotted on our automatic curve plotter and they are stored on tape as an input to second program that calculates thermo-elastic stress.

The thermo-elastic stress program has been obtained from Professor Christian of M.I.T. and is his program called FEAST. This converts temperature and pressure into mechanical stress and strain. The modification that we have done to this program is to adapt it to run on our computer. Also, the output of this program has been arranged so that it can be delivered to the curve plotters.

The third program is designed to present portions of the output data in graphical form using automatic curve plotting equipment. This program enables us to select the strain or the stress in any direction for plotting and also enables us to superimpose a number of different sections or planes through the rock on a single curve for comparison.

The combination of these programs into a single functioning unit is, we believe, a unique capability in that we now can start with any heat flux or temperature distribution and derive the resulting mechanical stress and strain in a body.

In its most general form, the program requires a large number of elements for the finite element matrix. In the problems, we have solved, we have reduced the complexity by assuming only a 100 element matrix having radial symmetry. That is; the incident radiation is either along the axis or along an annulus symmetrical about the axis. The rock is also assumed to be isotropic.

One simple problem that has been run will now be described to illustrate the form of the calculation. This is a single point of radiation on the axis of a block of quartzite. The laser incident power was 10,000 watts in a circular element .5 cm in diameter. The radiation time was varied from 2 to 50 msec in steps. The output of the computer is shown in Figure 18. This figure shows that the surface reached about 1500°C in 2 msec and reached the boiling point in 4 msec. Subsequent to that, the diffusion of the heated spot radially is shown by the spreading of the small

TEMPERATURE
100 °K

TIME = 4·50 × 10⁻³ SEC

TIME = 2 × 10⁻³ SEC

RADIUS
MM

15 mm BELOW SURFACE

SURFACE
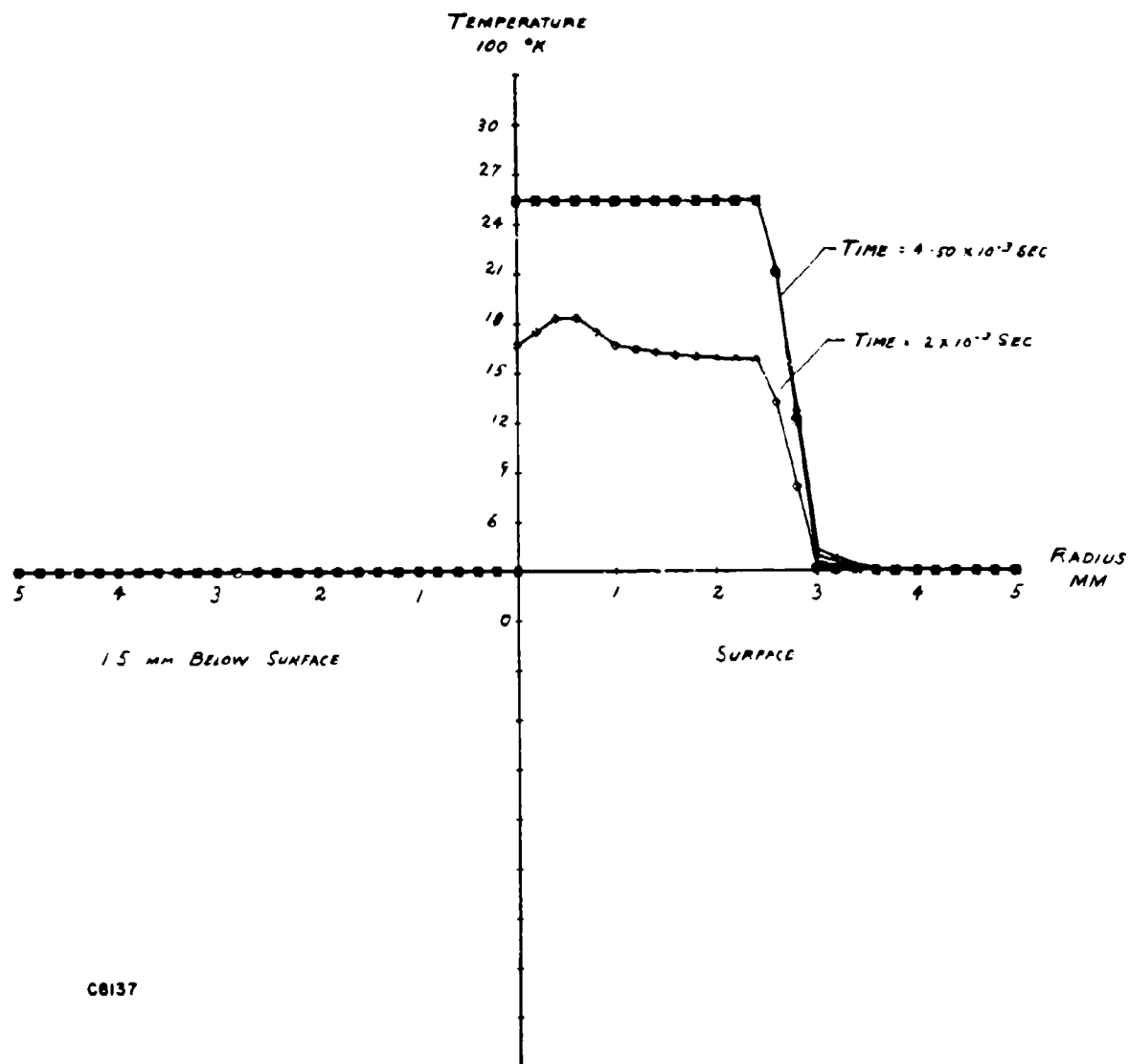
C6137

Figure 18   Computer plot of temperature profiles at various times
during the irradiation of a block of quartzite by a 10, 000
watt continuous wave laser focussed on a 5 mm diameter
spot.

tail exhibited near .3 cm radius. At .15 cm below the surface, there is
not sufficient temperature rise to be seen on the scale of the figure,
although the computer print-out contains information. The small bump in
the temperature curve around .05 cm is the result of the finite element
computer method and not a property of the rock.

These temperature profiles are then used as inputs to the FEAST
program. The stress pattern for the above temperature conditions are
displayed in Figure 19. The right side of the figure represents the stress
at the surface for the various times of radiation. The lower stress
corresponds to the first 2 msec of radiation and the other stresses result
from 4 to 50 msec. On the left-hand side of the figure, the stress is shown
at .15 cm below the surface. Recall that at this depth, the temperature is
much too low to be seen on the scale used in plotting Figure 18. Nevertheless,
the stress is clearly above the fracture limit for quartzite. This figure
shows that in the region of the radiation, at the surface, the material is
compressed, whereas outside of the region of radiation, both on the surface
and below the irradiated spot, it is in tension.

Since rocks are about an order of magnitude weaker in tension than
in compression, failure of the rock occurs outside the irradiated region
where the tension exceeds the critical tensile stress for failure.

The physical properties of the quartzite, granite and basalt that have
been used with this computer program are given in Table III. The actual
values were taken from recently published sources[4] as being typical of the
type of rocks on which experiments were done.

Our computer program allows both the elastic modulus and the
thermal conductivity to be represented as a function of temperature.
For the elastic modulus, the values at room temperature (300°K) is
introduced and also the modulus is set equal to zero at the melting
point. The computer program interpolates the modulus of every
element linearly as a function of the elements temperature between these
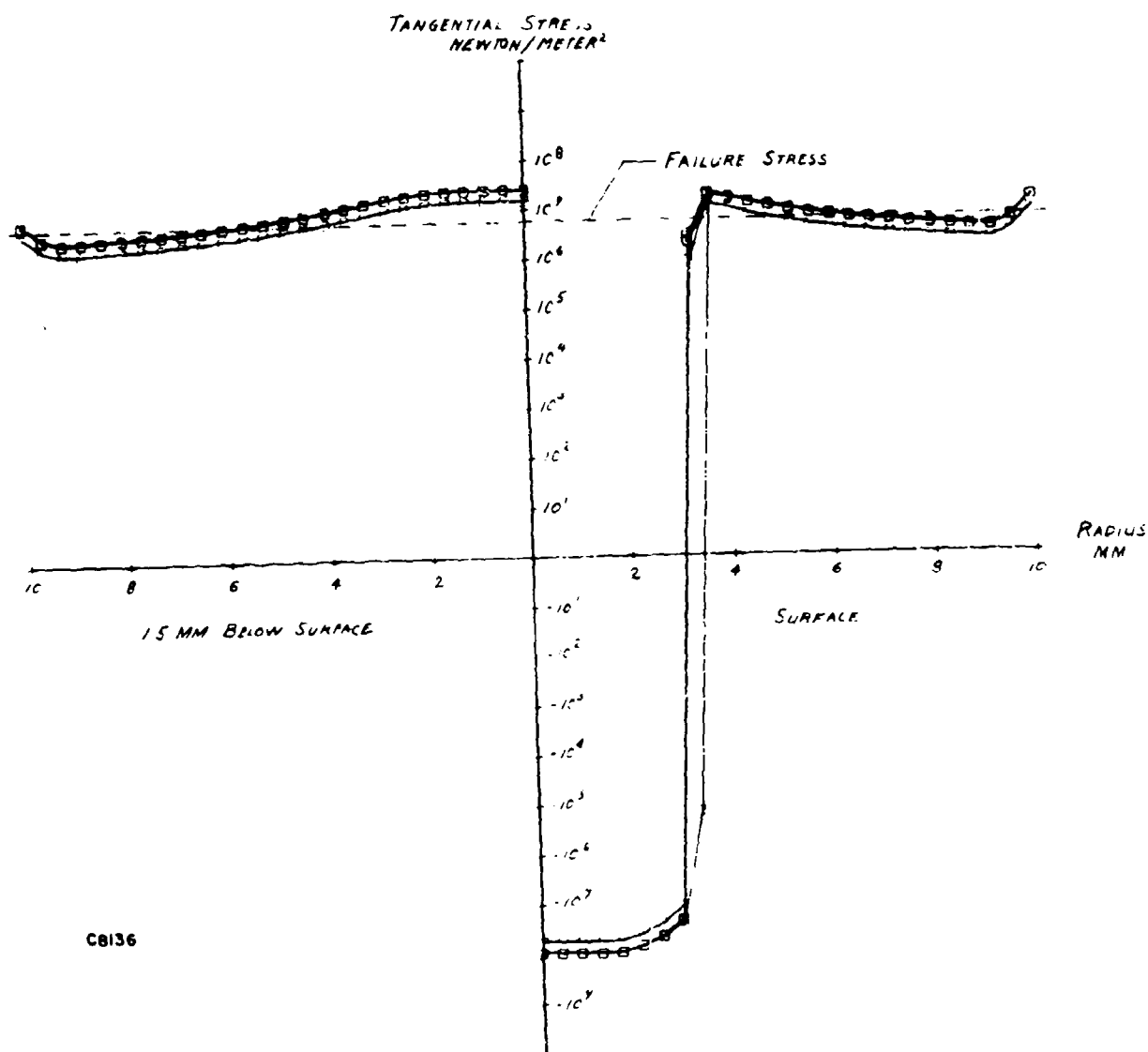two points in solving the stress-strain matrix. In the calculations that were

Figure 19   Computer plot for the stress conditions produced in quartzite
rock by the irradiation shown in Figure 10. This shows that
a failure zone extends far beyond the irradiated region. Note
that stress is plotted on a log scale.

TABLE III

ASSUMED PROPERTIES OF ROCK FOR COMPUTATION

	Quartzite	Granite	Basalt
Density kg/m^3	2.64×10^3	2.72×10^3	2.97×10^3
Poisson's ratio	.15	.26	.24
Melting point	2000.	1550.	1550.
Modulus of elasticity at $300^{\circ}K$ n/m^2	10^{11}	10^{11}	10^{11}
Modulus of elasticity at melting point n/m^2	0	0	0
Tensile fracture stress n/m^2	1.45×10^7	1.45×10^7	1.45×10^7
Thermal conductivity coefficient A,	7.0×10^{-4}	8.0×10^{-4}	1.45×10^{-5}
Thermal conductivity coefficient B	-1.13	-.667	-.15
Coefficient of thermal expansion deg^{-1}	1.1×10^{-5}	8×10^{-6}	5.4×10^{-6}

presented in the six month interim report, this feature of the program was not present. The modulus was assumed constant over all temperature. This resulted in a rock with an unrealistically high thermal stress. The present calculations allow the rock to be progressively weaker where it is heated and come closer to modeling actual rocks. At some future time, if more detailed information is available concerning the elastic properties at various temperatures, the same program can be used with more than two points for the temperature-elastic modulus interpolation. The thermal conductivity of rocks is also a function of temperature being higher at low temperatures. For the basic data, the report by Marovelli and Veith[5] was used. The data in this report was plotted against temperature using a log-log plot. Over most of the temperature range, this experimental data could be represented by straight lines on the plot. Basalt had the lowest slope giving a temperature conductivity substantially independent of temperature. Quartzite had the largest slope and at low temperature had the largest thermal conductivity. Granite was intermediate between the two. From these slopes, the thermal conductivity was approximated by an exponential function having the form $k = A T^B$, where A and B are constants and T is expressed in $^\circ K$. Table III gives the physical constants of the rocks that were entered into the computer program.

The type of problem that was investigated with the thermal-elastic stress computer program was the receipt by a rock face of an annulus of laser radiation. The laser flux was allowed to be incident on a single circular node at a specified radius in quartzite and basalt rocks having the properties described in Table III. The intensity was chosen so that the temperature at the surface did not reach the melting point. The stress levels generated by this radiation were studied as a function of exposure time, radius of the circle, and rock type. The computer output was fed to an automatic curve plotter and the values of temperature, radial component of stress, and tangential stress component were plotted against various positions in the rock. The failure stress was taken at 1.45×10^7 newtons/m^2 (2100 lbs/in.^{2}) intension for both quartzite and basalt.

One typical problem that was calculated is illustrated in Figures 20, 21, 22. This is Test Number 1328B in which 15,000 watts was allowed to fall on basalt in an annulus at a radius of 36 centimeters for up to 70 seconds. A characteristic of the finite element method used in the thermal-elastic stress calculation is that the radiation is received at nodal points. Because of the circular symmetry of the calculations these nodes are really circles about the origin. For this particular problem, fifteen thousand watts of radiation was received at a nodal point radius of 36 cm. Other nodal points appear at a radius separation of 4 cm. In performing the calculation, the incident radiation is considered to be uniformly distributed on the two faces of the rock sample on either side of the node for a radial distance of a half nodal spacing. In other words, the incident radiation is considered by the computer program to be uniformly distributed over a rock face centered about the nodal point radius and having a width of one nodal spacing. This is very nearly the same calculation that would result from a Gaussian distribution of incident energy with the same half width. Figure 20 shows the temperatures that were reached. On the right side of the figure is plotted the temperature at the surface. This finally reached about 750°K. On the left side of this figure is plotted the temperature at a depth of 1.5 cm. This shows that a very small temperature rise occurred at this depth, about 25°C. Thus we have the entire zone of heating confined to this annular ring within about a centimeter of the surface.

Figure 21 shows the tangential component of the stress plotted after 70 seconds. Inside the heated annulus, the rock is in tension. At the heated zone, it is in compression down to a depth of about 2 cm and outside the heated zone it is again in tension. There is a substantial tensile component of stress down to a depth of about 4 cm. Considerably deeper than the zone of heating.

The radial component of stress is plotted in Figure 22. This shows a similar pattern except that the region of compression is at a slightly larger radius than for the tensile component. When one examines the computer printout directly, where the maximum stress is printed one can conclude that failure of the rock would occur out to a radius of 37.5 cm and a depth of 2.7 cm after 30 seconds radiation. If this results in a spall of a disc of these dimensions, 4.5×10^5 joules would be consumed in the

Figure 20   Computer analysis of annular beam on basalt at 36 cm radius
Beam power 15,000 watts.   The surface temperature reached
$750^{\circ}K$ in 70 seconds. At a depth of 1.5 cm only a slight
temperature rise is observed.

TEST NO. 1328B ANNULUS BASALT, 15000WATTS R= 36 cm

T STRESS PLOT
TIME= 70 sec

Figure 21   The stress resulting from the exposure of Figure 20 plotted
here is the tangential stress after 70 seconds at various depths
in the rock.

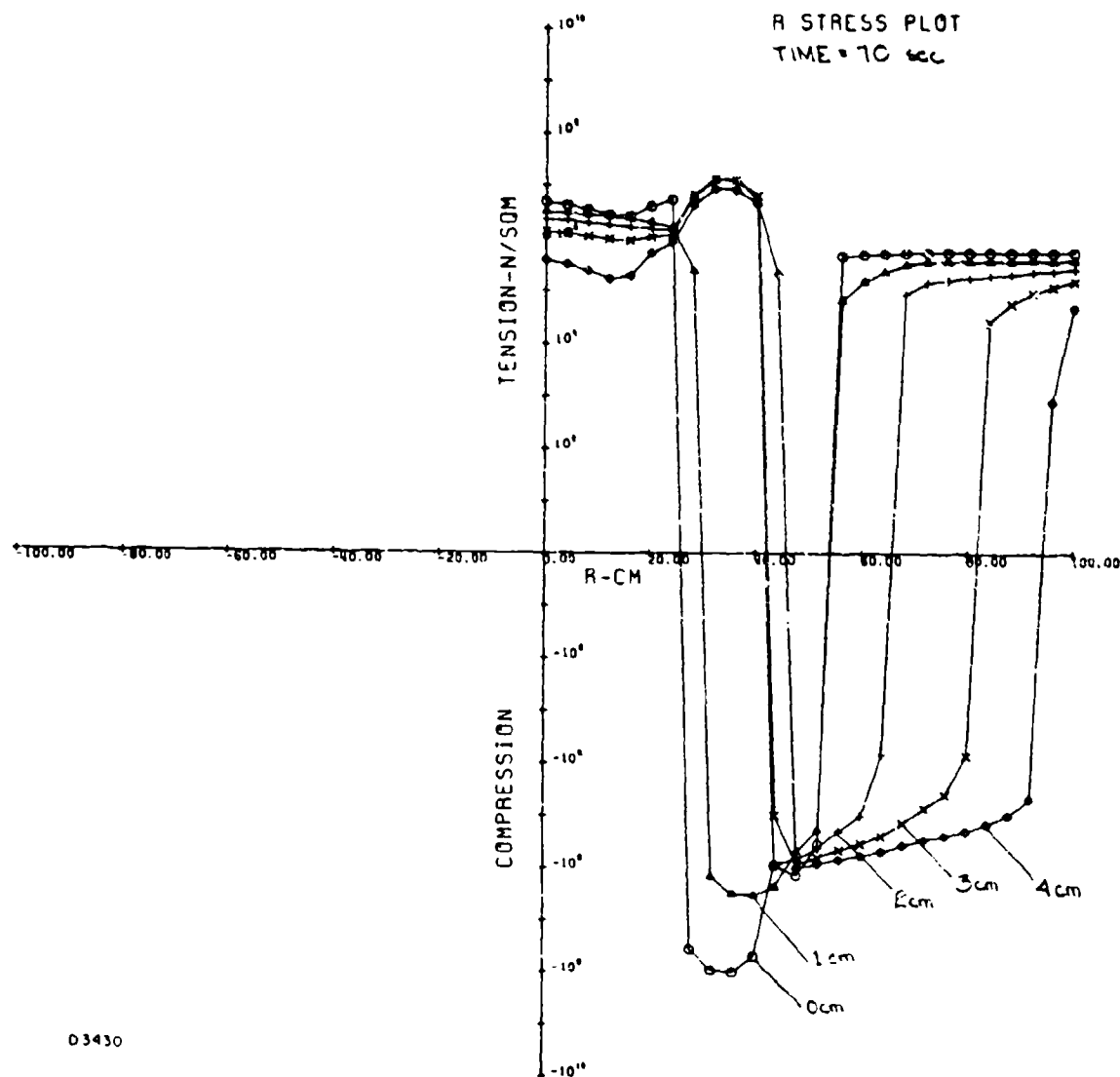TEST NO. 13288 ANNULUS BASALT. 15000WATTS R=36cm

Figure 22   The same exposure as Figure 20. Here the radial component
of stress is plotted. Failure stress in tension extends to a
depth of 3 cm.

-75-

removal of 1.19×10^4 cm^3 of rock by spalling with a specific energy of 37.8 joules/cm^3.

Examples were run for different conditions and the results of the various computer calculations, after evaluation are presented in Table IV.

For each type of problem, the shortest radiation time was found which resulted in a maximum stress larger than the assumed failure stress. The energy and extent of failure is given in Table V. The right hand column of this table gives the calculated values of specific energy for rock removal in j/cm^3. This shows that the specific energy is:

1. Substantially independent of the radius of heating
2. About 2.5 times larger for basalt than for quartzite being about 45 j/cm^3 for quartzite and 110 j/cm^3 for basalt

These results can now be compared with the experimental values for the spalling of rocks heated in the form of an annulus, and presented in Figure 17 the map of specific energy for rock removal and in Table II. The spalled experiments are contained on the left hand part of this map where the lower values of incident intensity are plotted.

The computer calculations are supported by the experimental evidence. In the first place, quartzite is more easily spalled than basalt. Secondly the specific energy for rock removal is only weakly dependent on the diameter of the experiment. However, the experiments show two orders of magnitude higher specific energy than the computer runs. For example, the calculations show a specific energy of about 40 j/cm^3 required to spall quartzite. In the experiments numbers 236-244, done with quartzite, the experimental values of energy for spalling was from 12,000 to 14,000 j/cm^3. The computer program predicted a specific energy for spalling basalt of about 110 j/cm^3. In experiments 254 and 255, about 65,000 j/cm^3 was actually required.

There are a number of ways to explain why the experimental values are so much larger. Laser induced surface temperature can be very high but thermal-elastic stress is most efficiently generated from large regions which are heated only a few hundred degrees above the main mass. The computer program represents an ideal case. Wherever the stress exceeds an assumed failure stress, we concluded that the rock would be cracked away

-76-

TABLE IV

CALCULATION OF FAILURE OF A HEATED ANNULUS

Failure stress assumed equal 1.45×10^7 n/m^2

Case No.	Rock	Radius of Heating (cm)	Power (watts)	Time (sec)	Depth of Failure (cm)	Radius of Failure (cm)	Volume (cm^3)	Energy (joules)	Specific Energy (j/cm^3)
1324	Q	4.0	3000	0.2	0.30	3.75	13.25	6.0×10^2	45.3
1324	Q	4.0	3000	0.8	0.90	3.75	39.70	2.4×10^3	60.4
1329	E	3.8	3000	0.2	none	none	-	6.0×10^2	-
1329	B	3.8	3000	0.8	0.51	3.75	22.5	2.4×10^3	106.5
1329	B	3.8	3000	2.0	0.87	3.75	38.4	6.0×10^3	156.1
1327	B	3.8	1500	0.6	none	none	-	9.0×10^2	-
1327	B	3.8	1500	2.4	0.66	3.75	29.2	3.6×10^3	123.5
1327	B	3.8	1500	6.0	1.05	3.75	46.4	9.0×10^3	194.0
1325A	Q	11.0	6000	2.0	none	none	-	1.2×10^4	-
1325A	Q	11.0	6000	6.0	1.95	11.2	768.	3.6×10^4	46.8
1325A	Q	11.0	6000	20.0	3.25	11.2	1281.	1.2×10^5	93.7
1328	B	11.0	3000	1.0	none	none	-	3.0×10^3	-
1328	B	11.0	3000	3.0	none	none	-	9.0×10^3	-
1328	B	11.0	3000	10.0	none	none	-	3.0×10^4	-
1328A	B	11.0	6000	2.0	none	none	-	1.2×10^4	-
1328A	B	11.0	6000	6.0	0.8	11.2	315.	3.6×10^4	114.?

Case No.	Rock	Radius of Heating (cm)	Power (watts)	Time (sec)	Depth of Failure (cm)	Radius of Failure (cm)	Volume (cm³)	Energy (joules)	Specific Energy (j/cm³)
1325B	Q	36.	15,000	10.	none	none	-	1.5×10^5	-
1325B	Q	36.	15,000	30.	2.7	37.5	1.19×10^4	4.5×10^5	37.8
1325B	Q	36.	15,000	70.	4.4	37.5	1.94×10^4	1.05×10^6	54.0
1328B	B	36.	15,000	10.	none	none	-	1.5×10^5	-
1328B	B	36.	15,000	30.	0.22	42.5	1248.	4.5×10^5	360.0
1328B	B	36.	15,000	70.	3.0	32.5	9955.	1.05×10^6	105.0

TABLE V

MOST EFFICIENT CALCULATION FOR EACH PROBLEM

Failure stress assumed equal 1.45×10^7 n/m^2

Case No.	Rock	Radius of Heating (cm)	Power (kw)	Time (sec)	Depth of Failure (cm)	Radius of Failure (cm)	Volume removed (cm³)	Energy (joules)	Specific Energy (j/cm³)
1324	Q	4.0	3.	0.2	0.3	3.75	13.25	6.0×10^2	45.3
1325A	Q	11.0	6.	6.0	1.95	11.2	768.	3.6×10^4	46.8
1325B	Q	36.0	15.	30.0	2.7	37.5	1.19×10^4	4.5×10^5	37.8
1329	B	3.8	3.	0.8	0.51	3.75	22.5	2.4×10^3	106.5
1327	B	3.8	1.5	2.4	0.66	3.75	29.2	3.6×10^3	123.5
1328A	B	11.0	6.	7.0	0.8	11.2	315.	3.6×10^4	114.3
1328B	B	36.0	15.	70.	3.0	32.5	9955.	1.05×10^6	105.0

and fall free. In an experiment even though small cracks are produced, the rock is not completely freed. Spallation is not observed until the cracks enlarge sufficiently to enable pieces of rock to fall away. In the meantime, the rock sample continues to be heated. The surface can become so hot that the elastic modulus is small. Continued heating is then ineffective in producing additional thermal-elastic stress, but does contribute a large amount to the total energy consumption. If one wishes to get a high efficiency from induced thermal-elastic stress, the heat flux per unit area should be reduced considerably below the values used in our experiments.

It is quite clear, therefore, that to use the full potential of the laser, experiments must be done on a much larger scale with larger rock samples and much higher linear velocity of motion of the laser spot. This is one direction to pursue in future work.

A second important change in the experiment would be to use a laser that can be alternately switched between the continuous and pulsed mode. Thus, small cracks induced by the thermal-elastic stress could be enlarged by pressure pulses induced when laser energy is deposited below the surface in the crack itself.

VII. APPLICATIONS

It is clear that high power lasers are not efficient in merely drilling through rock. The experiments that we have done show between 1, 000 and 10, 000 joules required per centimeter of penetration for holes only a few centimeters deep. Furthermore, attempts to penetrate through large sections of rock show an even larger specific energy consumption. Theoretical work, so far unpublished, shows that there is a strong absorption of the laser energy in the gases generated within a hole. This leads to a maximum depth of penetration for any given hole diameter. Attempts to penetrate beyond this value, result, according to our calculations in hole broadening and a very slow increase in the depth and the consumption of very large amounts of energy. Furthermore, above the hole, there is considerable smoke which also serves as an absorber of radiation. If the beam intensity is reduced to the point where rocks are spalled, the tests and computer runs with the laser shows that considerably higher efficiency is reached in rock removal. However, specific energies of between 10, 000 and 100, 000 joules per cubic centimeter are required for spalling.

In the above types of interactions, the laser is used primarily as a heat source. The unique properties of the laser, namely extremely high intensity at the focal point, and the ability to move the point of application of heat with great speed and control are not being used.

Research in connection with other projects has led us to conclude that it is very likely that cracks can be generated, and propagated with high efficiency when suitably focused laser radiation is moved with great speed over the surface of brittle solids. This result has not yet been demonstrated experimentally. However, we would like to consider what useful applications would result if one could produce and lead cracks with efficiency.

One application would be to produce a deep cored hole penetrating several feet into the rock, a few inches diameter. This gives us a powerful diagnostic tool. For example, a deep hole certainly will reveal the presence of water behind a tunneling face. If water comes out of the hole it can easily be plugged. Also, a hole of this nature may enable us to determine the consolidation of the formation. Suppose that a jack is placed in the hole and a stress-strain curve taken on the rock formation. If it is finely jointed, or loose, the formation will yield at low stress. If it is a consolidated, massive rock formation, the stress-strain curve will be quite stiff. Therefore the ability to drill cored holes without causing surface cracks and without using a great deal of time and energy, is certainly a consideration in speeding up the progression of a tunnel.

The second application is in the rock removal itself. Suppose that one has already determined that the tunnel face can be advanced with safety. It should then be possible to direct the laser in such a way as to crack out large boulders, each of a convenient size for eventual removal from the working face. When this is done, with the operator located at a distance from the tunnel face, in the comparative safety of an enclosed cabin, and without the need for explosives, we believe that the speed, safety and effectiveness of tunnel driving can be considerably improved. We hope that future work can be undertaken to explore the rapid and dynamic interaction of the laser with the rock through the production and reinforcement of elastic waves.

REFERENCES

1. Maurer, W. C., "Novel Drilling Techniques," Pergamon Press (1968).

2. Longhurst, R. S., "Geometrical and Physical Optics," Longman Press (1967).

3. Gerry, E. T., "Gas dynamic lasers," IEEE Spectrum, Vol. 7, pp. 51-58, Nov. 1970.

   Reilly, J. P., "Single-mode operation of a high-power pulsed N_2/CO_2," this issue, pp. 136-139.

   Locke, E. V., Hella, R. A. and Westra, L., "Performance of an unstable oscillator on a 30 kW CW GDL," IEEE J. Quantum Electron. (Corresp.), Vol. QE 7, pp. 581-583, Dec. 1971.

4. Thirumalai, K., "Twelfth annual symposium on rock mechanics," Chapter 36, AIME, New York (1971).

   Clark, S. P., Editor, "Handbook of Physical Constants," Geological Society of America (1966).

5. Marovelli, R. L. and Veith, R. F., Bureau of Mines R16604 (1965).